JSR Journal of Sedimentary Research
SEPM | Society for Sedimentary Geology

doi:10.2110/jsr.2023.066

1926 SEPM Society for Sedimentary Geology

Online 9 April 2024

Detrital Zircon U-Pb and (U-Th)/He double dating provenance signatures in the Jaca foreland basin: Interplay of direct vs recycled sources during Pyrenean orogenic growth

Xavier Coll[1]; David Gómez-Gras[1]; Marta Roigé[1]*; Daniel Stockli[2]; Antonio Teixell[1]; Salvador Boya[1]

[1]Departament de Geologia, Universitat Autònoma de Barcelona, 08193 Bellaterra, Spain

[2]The University of Texas at Austin, Department of Geological Sciences, Austin, TX 78712, USA

(*) Corresponding author

ABSTRACT

The Eocene to Miocene clastic wedge of the south Pyrenean basin constitutes a reference model to understand the progressive evolution of sediment provenance and source-to-sink dynamics in a foreland basin. We present new detrital zircon (DZ) U-Pb and U-Pb-He (ZHe) double dating data from the Jaca basin and the Ebro basin, providing insights into the evolution of the sedimentary systems that record a major tectonic and drainage reorganization from the late Eocene to Miocene. Three distinct DZ U-Pb signatures have been identified: (i) Variscan dominated; (ii) mixed Cadomian-Variscan; (iii) Cadomian dominated; and two DZ ZHe signatures (i) Pyrenean dominated; (ii) pre-Pyrenean dominated. Coupling DZ U-Pb, ZHe, and petrographic data allows us to discriminate among distinct Pyrenean sources as well as to understand how DZ signatures are propagated in a source-to-sink system. Our results indicate that while the eastern Jaca basin was fed from eastern source areas located in the central and eastern

Pyrenees, the western Jaca basin was fed from the Basque massifs and the Urbasa-Andía Sierra (Basque-Cantabrian Pyrenees).

INTRODUCTION

Sedimentary provenance analyses are key to deciphering source-to-sink patterns and the links between tectonics and sedimentation, particularly in foreland basins related to collisional orogens (Dickinson 1970; Steidtmann and Schmitt 1988; Garzanti et al. 2004). Foreland basins record the erosional and exhumational history of their source areas, providing valuable insights into the chronology of the deformation and unroofing of the related orogen (Fosdick et al. 2015; Labaume et al. 2016; Thomson et al. 2017; Odlum et al. 2019).

Detrital zircon (DZ) U-Pb and (U-Th)/He double-dating allows us to obtain crystallization and cooling timing constraints of the source areas feeding the basin. Since zircon is one of the most ubiquitous heavy minerals in crustal rocks, being highly resistant to weathering and diagenetic processes, DZ signatures have become a powerful and widely-applied provenance tool worldwide in the last decades (Reiners et al. 2005; Nie et al. 2012; Saylor et al. 2012). However, the resolution of this kind of studies might be limited due multiple source areas with similar or monotonous DZ age distributions, and recycling and/or cannibalization of older siliciclastic sedimentary rocks that might bias the reconstruction of the source area (Dickinson et al. 2009; Garzanti et al. 2013). Although extensive literature deals with the U-Pb signatures of direct sources, the role of sediment recycling in the propagation of DZ signatures is poorly constrained (Schwartz et al. 2019). Therefore, it is crucial to integrate as many provenance tools as possible (i.e., sandstone petrography, heavy mineral analysis, detrital geochronology and detrital thermochronology) in order to decipher the true complexity of the study case (Thomson et al. 2019; Coll et al. 2022).

Due to its extraordinarily well-preserved sedimentary record, the South Pyrenean basin is a reference model for foreland basins worldwide. The Lutetian to Miocene deposits of its western part -known as the Jaca basin- provide an excellent natural laboratory to study sediment recycling as well as the interplay between active source areas and sediment routing (Michael 2013; Thomson et al. 2017; Roigé et al. 2016; Roigé et al. 2017; Coll et al. 2020; Coll et al. 2022).

The paleogeography of the South Pyrenean basin has been well established from several works that have studied its stratigraphy, sedimentology and tectonics (e.g. Soler-Sampere and Puigdefàbregas 1970; Puigdefàbregas 1975; Mutti 1985; Barnolas and Teixell 1994; Payros et al. 1999; Oms et al. 2003; Remacha et al. 2005; Labaume et al. 2016; Oliva-Urcia et al. 2019; Vinyoles et al. 2021), as well as from provenance studies focused on the clastic infill (Fontana et al. 1989; Gupta and Pickering 2008; Caja et al. 2010; Whitchurch et al. 2011; Filleaudeau et al. 2012; Michael 2013; Roigé et al. 2016; Gómez-Gras et al. 2017; Roigé et al. 2017; Thomson et al. 2017; Coll et al. 2020; Coll et al. 2022). All this research allows us to constrain the occurrence of distinct axially-fed eastern-sourced systems mainly supplied by Paleozoic basement rocks and Mesozoic carbonates from the central and eastern Pyrenees (i.e. Roigé et al. 2016). During the early foredeep stages of the basin, the Hecho Group turbidites (early Eocene-middle Eocene) were fed through these axially east-sourced systems (Mutti et al. 1972). However, the activity of the Gavarnie and Guarga thrusts (Fig. 1) uplifted these turbidite deposits and promoted their erosion during Priabonian to Miocene times, which were recycled into transverse-fed north-sourced alluvial systems (Campodarbe and Bernués Formations) of the southern Jaca basin (Puigdefàbregas 1975; Teixell and García-Sansegundo 1995; Labaume et al. 2016; Roigé et al 2016; Roigé et al. 2017; Coll et al. 2022).

In the eastern Jaca basin, the provenance of the sedimentary systems is well constrained by sandstone petrography and heavy mineral analysis (Roigé et al. 2016; Roigé et al. 2017; Coll et al. 2020; Coll et al. 2022). Nonetheless, provenance studies using DZ signatures are only focused on the northern margin deposits (Roigé 2018). By contrast, in the western Jaca basin, the provenance of the late Eocene-Miocene siliciclastic systems is poorly constrained (Puigdefàbregas 1975; Payros et al. 1997; Astibia et al. 2005), and no quantitative data exists regarding sandstone detrital modes, heavy minerals, and DZ geochronologic signatures.

Our study aims to investigate the impact of the major reconfiguration of the catchment areas by applying DZ U-Pb and ZHe analysis in the southern margin and western area of the Jaca basin and the Ebro basin. This is the first-time applying U-Pb and ZHe double dating in the non-volcanic detrital zircons of the Jaca basin. In this work we (1) characterize the DZ U-Pb signatures recorded by deltaic, fluvial and alluvial fan systems of the eastern and western Jaca and Ebro basins, (2) characterize the zircon (U-Th)/He provenance signatures to constrain the exhumational history of the source areas, (3) compare these results with the more proximal, time equivalents of the nearby Ainsa and Tremp-Graus basins.

Our work has important applications to collision orogens where different source areas can produce similar compositional signatures, by contributing to the knowledge of the propagation and interplay of DZ signatures during recycling processes. This study also highlights the importance of integrating these techniques with petrographic data, in order to constrain sediment provenance and sediment dispersal patterns, and to avoid biased interpretations or undesired low resolution.

GEOLOGICAL SETTING AND STRATIGRAPHIC FRAMEWORK

The Jaca basin constitutes the western part of the South Pyrenean prowedge foreland basin (Fig. 1). From the late Cretaceous to early Miocene, the Eurasian and Iberian plate collision led to the formation of the Pyrenean fold-and-thrust belt, which grew diachronously as a result of the oblique character of the collision (Puigdefàbregas et al. 1992; Teixell et al. 2018; Vergés et al. 2002; Mouthereau et al. 2014). The core of the belt (known as the Axial Zone) is made of basement-involved stacked thrust sheets, flanked to the north by the North Pyrenean Zone (where the pre-collisional rift axis is still preserved; Lagabrielle et al. 2010; Fig. 1A). The Cenozoic sedimentary deposits that occur further north constitute the retro-wedge foreland basin (Aquitanian basin). In the South Pyrenean Zone, the deformation was accommodated by an imbricate thrust fan (Cámara and Klimowitz 1985; Labaume et al. 1985; Teixell 1996; Labaume et al. 2016; Muñoz et al. 2018), which in the-west central Pyrenees is constituted by four main thrust sheets. From north to south, these thrust sheets are: (a) the Lakora-Eaux-Chaudes, (b) the Gavarnie, (c) the Broto, and (d) the Guarga thrusts (Fig. 1B). These thrust sheets involve the Paleozoic basement, a pre-alpine Paleozoic and Mesozoic sedimentary cover, and a late Cretaceous to early Miocene foreland basin, which is bordered to the south by the External Sierras thrust front. To the south, the Ebro basin records the final stages of the Pyrenean exhumation (i.e. Hirst and Nichols 1986; Rat et al. 2022). At the western edge of the Pyrenees the Basque massifs (Fig. 1A) constitute the junction of the Pyrenees-Cantabrian orogenic system (Lescoutre et al. 2020 and references therein). These massifs are composed by Paleozoic rocks overlain by Permian to Cretaceous rocks which are mainly represented by sedimentary deposits.

The Axial Zone is constituted by Paleozoic rocks, which are mainly represented by (a) upper Neoproterozoic to Permian sedimentary rocks (i.e. Margalef et al. 2016), (b) Cambro-Ordovician gneisses and Carboniferous-Permian granitic rocks and (c) Cambrian to Devonian low-grade metamorphic rocks (Capaldi et al. 2022, and references within). These Paleozoic rocks are unconformably overlain by Permo-Triassic red beds or Cretaceous limestones. The pre-orogenic Mesozoic succession in the South Pyrenean thrust sheets includes the Triassic Keuper facies, which are involved in thrust sheet propagation, acting as an evaporite detachment level during extension and contraction, and featuring salt diapirism processes in the central Pyrenees (Saura et al. 2016; Burrel and Teixell 2021; Burrel et al. 2021; Hudec et al. 2021). The rest of the succession is made up of thick Jurassic-Cretaceous carbonate and sandstone-shale successions. The South Pyrenean foreland basin is an assemblage of synorogenic rocks, related to the late Santonian-early Miocene shortening, that recorded a major drainage reorganization in the mid-late Eocene: the progression of the fold-and-thrust belt deformation triggered a shift from a predominantly axial drainage network to a series of transverse systems (Whitchurch et al. 2011). This shift was expressed by the fluvio-deltaic environments of the Àger and Tremp-Graus basins (eastern sector of the South Pyrenean basin, Fig. 1A) that funneled sediments to the west, where the slope and deep-marine environments of the Ainsa and Jaca basins (the Hecho Group turbidites) developed during the underfilled foreland basin stage (Nijman and Nio 1975; Mutti 1985; Bentham et al. 1992; Caja et al. 2010). With the growth of the orogen, these environments were progressively replaced from east to west, during the mid to late Eocene, by deltaic deposits, and by fluvio-alluvial environments during Oligocene-Miocene times (Graus, Campodarbe and Bernués Formations.) (Puigdefàbregas 1975; Dreyer et al. 1999).

The Eastern Jaca Basin

The end of the turbiditic sedimentation (Hecho Group turbidites; early Eocene-middle Eocene) in the Jaca basin was followed by mixed deltaic and fluvial environments (Puigdefàbregas 1975). In the eastern Jaca basin, the first deltaic system is represented by the Sabiñánigo Sandstone Formation (Bartonian) which prograded from east to west (Mangin 1960). The stratigraphic section continues with the Pamplona Marls Formation (Figs. 2, 3), which constitutes the prodelta deposits of the Belsué-Atarés deltaic Formation (Puigdefàbregas, 1975). During the Bartonian-Priabonian, the Belsué-Atarés delta prograded from east to west sourced from the central and eastern Pyrenees (Roigé et al. 2017; Coll et al. 2021). Towards the north-western part of the basin, the Belsué-Atarés Formation passes to the Priabonian Martés and Güendulain Formations (Puigdefàbregas 1975). All these deltaic environments were progressively substituted by the fluvial to alluvial Campodarbe Formation (Bartonian-Chattian; Puigdefàbregas 1975; Boya 2018; Roigé et al. 2019), which marked the endorheic basin stage and the onset of terrestrial sedimentation throughout the entire basin at 36 Ma (Barnolas and Gil-Peña. 2001; Costa et al. 2010; Ortí et al. 1986; Payros et al. 2000).

The Campodarbe Formation (Mutti et al. 1972) is a fluvial to alluvial succession (Bartonian-Chattian), where at least two main sediment routing systems can be identified (Puigdefàbregas 1975). In the northern margin, an east-derived axial fluvial system, entering the Jaca basin through the southeastern margin, interacted with a north-derived transverse alluvial fan system, mainly controlled by the activity of the Gavarnie thrust, and mostly derived from the recycling of the former lower to middle Eocene Hecho Group turbidites (Puigdefàbregas 1975; Roigé et al. 2016; Roigé et al. 2017; Coll et al. 2020). By contrast, the sedimentation in the southern edge was dominated by two axially-fed fluvial systems sourced from the central and eastern Pyrenees (Coll et al. 2022), and strongly controlled by growing tectonic structures of the External Sierras (Puigdefabregas 1975; Jolley 1988; Hogan 1993; Hogan and Burbank 1996; Labaume et al. 2016; Labaume and Teixell. 2018). The last stages of the basin infill are marked by the Bernués Formation (Chattian-Aquitanian; Puigdefàbregas 1975; Arenas 1993; Roigé et al. 2019), a complex of alluvial fan deposits sourced from the north of the basin (Figs. 2, 3).

As the orogenic deformation progressed to the south, the External Sierras thrust front (Soler-Sampere and Puigdefàbregas 1970; Labaume et al. 1985; Teixell 1996; Oliva-Urcia et al. 2016;) became strongly emergent (Oligocene-Miocene), and split the Campodarbe Formation in the Jaca basin to the north from the Ebro basin to the south (Fig. 3). The activity of the Guarga thrust sheet triggered the formation of the north-derived Luna alluvial fan system, sourced from the recycling of the Jaca basin and the Axial Zone further north, and from the Basque massifs to the northwest (Puigdefàbregas 1975; Arenas et al. 2001; Roige et al. 2019).

The Western Jaca Basin

Towards the western sector of the Jaca basin, time-equivalent deposits are constituted, from base to top, by: the Ezkaba Sandstone Formation, the Pamplona Marls Formation, the Ardanatz Formation, the Illundain marls Formation, the Yesa turbidites, the Guendulain Formation, and the Campodarbe and Bernués Formations (Figs. 2, 3).

The Bartonian Ezkaba Sandstone Formation (western time-equivalent deposits of the deltaic Sabiñánigo Formation in the east; Puigdefàbregas 1975; Payros et al. 1997) is a channel-levee turbidite system developed at the base of the Bartonian-Priabonian Pamplona Marls Formation (Mangin 1960; Astibia et al. 2005) in the northwestern sector of the basin, and it is sourced from the Basque massifs (Payros et al. 1997). The Pamplona Marls Formation, the Ardanatz Formation (Bartonian) and the Bartonian-Priabonian Ilundain Marls Formation correspond to prodelta, delta front, and restricted platform environments that were related to the progradation of the Belsué-Atarés delta in the eastern Jaca basin (Puigdefàbregas 1975; Astibia et al. 2005; Astibia et al. 2014).

The Ardanatz Formation (Bartonian) is a set of flood-influenced delta-front sandstone lobes interbedded at the base of the Ilundain Marls Formation (Astibia et al. 2005). The general distribution of facies (shallow-water environments to the west and turbiditic channels to the east) suggests no link with the Belsué-Atarés delta (Puigdefàbregas 1975). To the east, another formation has been related to the progradation of the Belsué-Atarés delta, the Yesa turbidites (Priabonian), which occur at the top of the Pamplona marls (Puigdefàbregas 1975).

The Priabonian Güendulain Formation (Payros et al. 2000) constitute a series of coastal deposits divided in three distinct members: the lower evaporite, the middle sabkha marl, and the upper Liédena Sandstone Formation. The latter, constitutes a wavedominated delta containing the last deposits with marine influence in the Jaca basin (Puigdefàbregas, 1975).

The overlying Campodarbe and Bernués Formations (Bartonian to Miocene) represent the development of fully terrestrial fluvio-lacustrine and alluvial environments throughout the basin (Puigdefàbregas, 1975). In the Izaga syncline area, the Campodarbe Formation is constituted by lacustrine deposits (Zabalza facies; Puigdefàbregas 1975) until the irruption of the Izaga alluvial fan, sourced from northern areas comprising Paleocene-Eocene sedimentary rocks (Puigdefàbregas 1975).

GEOCHRONOLOGIC AND THERMOCHONOLOGIC CHARACTERIZATION OF POTENTIAL SOURCE AREAS

U-Pb Characterization of the Source Area

In order to comprehend the DZ U-Pb signatures from the Jaca basin, it is necessary to review the age signatures of the different possible sources. These can be the different tectonic domains of the central and western Pyrenees, which include Paleozoic metasedimentary and igneous basement of the Axial Zone and Basque massifs, the preorogenic Mesozoic sedimentary cover successions, and the early synorogenic late Cretaceous to middle Eocene deposits.

The clastic metasedimentary succession of the Axial Zone (Cambrian-Ordovician-Silurian-Devonian) displays DZ U-Pb signatures dominated by >700 Ma age modes, with an important Cadomian/Pan-African component (520-700Ma), and a subsidiary 420-520 Ma population (Hart et al. 2016; Margalef. 2016). Orthogneissic rocks of the crystalline core of the Pyrenees mainly yield Ordovician protolith ages ranging from 485 to 450 Ma

(Denèle et al. 2007; Martinez et al. 2011). Carboniferous strata contain dominant recycled Cambro-Devonian DZ signatures and syndepositional volcanic zircons of 325-360 Ma (Martínez et al. 2015; Hart et al. 2016). Variscan igneous plutons yield ages ranging from 280-315 Ma (Whitchurch et al 2011, and references within). Permo-Triassic clastic deposits display dominant Cadomian (520-700 Ma) and >700 Ma age components, with scarce Variscan ages (Hart et al. 2016). Permian and late Triassic mafic volcanic and subvolcanic rocks in the region are present but unlikely to significantly contribute with zircon grains. Cretaceous sedimentary rocks display different DZ U-Pb signatures depending on the location and the stratigraphic level. Scarce data available show that Variscan-dominated ages can be found in the clastic early and late Cretaceous deposits from the central and eastern Pyrenees (Filleaudeau et al. 2012; Thomson et al. 2016; Odlum et al. 2019) and North Mauleón basin (NPZ; Hart et al. 2016), whereas Cadomian-dominated occurs in the early Cretaceous of the Mendibelza massif (NPZ), in the late Cretaceous of the North Mauleón basin (Hart et al. 2016), and in the late Cretaceous Aren Formation (Central Pyrenees; Whitchurch et al. 2011) or Adraén Formation in the (Bagà area, Odlum et al. 2019). Moreover, Paleocene-Eocene Deposits of the south-central Pyrenean basin (Ainsa, Tremp, and Àger basins; Fig. 1) show variable DZ distributions, which reflect the provenance evolution experienced by these sedimentary systems, alternating dominant Cadomian and Cambro-Devonian ages with Variscan components trough time (Whitchurch et al. 2011; Filleaudeau et al. 2012; Thomson et al. 2017; Odlum et al. 2019; Thomson et al. 2019). Finally, Oligo-Miocene calc-alkaline magmatism reported from the Mediterranean basin related to the opening of the Valencia Gulf (Marti et al. 1992; Sabat et al. 1995) could supply Cenozoic syndepositional zircons through ash airfall(Roigé et al. 2019).

In addition to the different age modes displayed by the different rocks, their zircon fertility may also have an impact on the DZ populations (Moecher and Samson 2006; Dickinson 2008; Malusà et al. 2016). A qualitative approach to the Pyrenean case (Thomson et al. 2017) infers the highest zircon fertility for the Variscan granitoids, whereas in the fine-grained Cambro-Ordovician metasedimentary formations moderate fertility is expected (Hart et al. 2016). By contrast, Triassic sandstones (dominantly arkosic) might display a high zircon fertility as they were sourced from the crystalline basement. Cretaceous to Paleocene formations (mainly carbonates), are expected to have a very low zircon fertility, although siliciclastic sandstones might display moderate to high fertility. We assume that the Eocene clastic formations (including the Hecho Group turbidites) have moderate zircon fertility, depending on their contents of carbonate (low fertility) vs siliciclastic (high fertility) grains. Moreover, turbidite layers sourced from felsic igneous rocks will produce higher zircon fertility than those sourced from metasedimentary basement rocks, and zircons produced by fine-grained Paleozoic metasediments (Neoproterozoic-dominated) are expected to be smaller than those delivered from plutonic rocks (Variscan-dominated).

(U-Th)/He characterization of the Source Area

Pyrenean ZHe ages (20-85 Ma) record cooling related to Pyrenean shortening and exhumation during plate convergence and are restricted to the thermally reset Paleozoic igneous-metamorphic basement (Axial Zone and North Pyrenean Zone) exhumed during the Pyrenean Orogeny (Whitchurch et al. 2011; Filleaudeau et al. 2012; Thomson et al. 2017). Cretaceous ZHe ages (85-155 Ma) are related to rifting-hyperextension and the HT-LP metamorphism occurring along the Iberia-Eurasia divergent plate boundary

(Lagabrielle et al. 2010). Such ages have been found in the syn-rift sedimentary units of the Pedraforca thrust sheet and the inverted Organyà basin (Odlum et al. 2019), as well as in the late Cretaceous of the North Pyrenean Zone, where the pre-collisional rift architecture is still preserved (Bosch et al. 2016). Liasic ZHe ages (180-201 Ma) can be attributed to widespread ophitic magmatism and the magmatic episode associated with the central Atlantic magmatic province (Marzoli et al. 1999; Mothereau et al. 2014). Permo-Triassic (201-295 Ma) and Variscan (>295 Ma) ZHe ages can be attributed to non-reset zircon grains originally sourced from the former Ebro massif into the Cretaceous-Eocene South Pyrenean foreland basin (cratonic margin).

METHODOLOGY

Twenty-five sandstone samples (2-4 Kg) from seven stratigraphic profiles were collected in the field (see supplementary file S1). In order to avoid hydraulic-sorting effects that might bias the analytical results, medium-grained sandstones were targeted, avoiding locally reworked deposits (Malusà et al., 2016; Garzanti et al., 2008; Garzanti et al., 2009; Garzanti et al., 2019; Andò, 2020). In addition, samples from each depositional system were collected from similar facies to minimize hydraulic-sorting effects related to different processes within the same depositional environment.

Following standard heavy mineral separation methods, samples were crushed with a Retsch Disc Mill DM 200 and submitted to Struers Metason 200 ultrasound machine (5 minutes) to help desegregation of well-cemented sands and clay coatings. The <500µm window was obtained through dry sieving with a digital electromagnetic sieve shaker BA-200. The recovery of the heavy fraction was done in two steps, using a Holman-Wilfley laboratory shaker table, and by the centrifuging method (using nontoxic dense liquid Na-polytungstate; 3.10g/cm3) and partial freezing with liquid nitrogen (Andò, 2020). Finally, zircons were obtained using a Frantz isodynamic magnetic separation. Mineral separation was performed at the Thin Section Lab of the Department of Geology of the Universitat Autònoma de Barcelona.

Zircon U-Pb Geochronology

Zircon grains were mounted onto double-sided adhesive plastic pucks and left unpolished for depth-profile analysis (Campbell et al. 2005; Hart et al. 2017). For each sample, at least 120 zircons were selected randomly and analyzed using the laser ablation-inductively coupled plasma-mass spectrometry (LA-ICP-MS) U-Pb geochronology, in order to obtain a statistically robust and representative provenance dataset (Vermeesch, 2004). U-Pb analysis was performed using a PhotonMachine Analyte G.2 excimer laser with a HeLex 238 sample cell and a Thermo Scientific Element2 ICP-MS. GJ1 was used as a primary standard (Jackson et al. 2004), and Plesovice (Sláma et al., 2008) was used as a secondary standard, to obtain data quality control. A 30 µm laser spot ablated 15 µm deep pits on the flat prism plane of the zircon grains. Data were reduced using VizualAgeTM data reduction scheme for the IoliteTM on Igor ProTM software (Paton et al. 2011). During data reduction, individual analyses were deleted if the grains were not zircon or there was evidence of errors in analysis. 206Pb/238U ages are used for grains younger than 850 Ma, while 207Pb/206Pb ages are used for grains older than 850 Ma. Individual zircon ages were excluded if there was a 206Pb/238U 2σ error greater than 10%, or 206Pb/238U and 207Pb/235U discordance greater than 10% for grains younger than 850 Ma or 206Pb/238U age and 206Pb/207Pb discordance greater than 20% for grains older than 850 Ma. All the ages are presented with two sigma absolute errors.

Zircon (U-Th)/He Thermochronology

After U-Pb DZ signature characterization, ten samples were selected for (U-Th)/He DZ Analysis. Six to nineteen concordant single-age zircons free of uranium zonation (per sample) were targeted for double dating analysis, based on of U-Pb age components relative abundance and the criteria for (U-Th)/He analysis (Farley 2002; Saylor et al. 2012; Hart 2015; Hart et al. 2017). Grains were individually packed into platinum (Pt) foil packets and were heated and degassed under ultra-high vacuum. Total He concentration was measured on a quadrupole mass spectrometer. Completely degassed grains were removed from Pt packets and dissolved with a combination of Hf and HNO3. Dissolved grains were analyzed on a Thermo Scientific Element2 ICP-MS for absolute U, Th, and Sm concentrations (Wolfe and Stockli 2010). Fish Canyon Tuff zircons were run with unknown grains to monitor data quality (Reiners 2005). Astandard error of 8% was applied to all measurements. Each crystal was morphometrically measured for alpha-ejection corrections, following the equations from Farley et al (1996), and assuming a grain geometry and that the second grain width is equal to the width measured. Partially/fractured or completely broken grains during unpacking from Pt packets, as well as grains containing fluid inclusions, were excluded from the analysis. Incomplete dissolved grains were also excluded. All U-Pb and He analyses were conducted at the UTChron Laboratory at the University of Texas at Austin.

Statistical Analysis

We applied multi-dimensional scaling and correspondence analysis as exploratory compositional data analysis tools to assess similarities/dissimilarities between samples (Vermeesch 2013; 2018). Results are displayed as biplots to facilitate the visualization and results interpretation. Statistical treatment was done using the Provenance R-package (Vermeesch et al. 2016; Vermeesch 2018) and allowed the distinction between distinctive U-Pb and (U-Th)/He components signatures.

RESULTS

DZ U-Pb geochronological signatures

DZ U-Pb age populations (Table 1) are grouped into twelve U-Pb age components: Cenozoic (0-66 Ma), Late Mesozoic (66-180 Ma), Permo-Triassic (180-280 Ma), Late Variscan (280-310 Ma); Early Variscan (310-370 Ma), Cambro-Devonian (370-520 Ma), Cadomian (520-700 Ma), Neoproterozoic (700-900 Ma), Kibaran (900-1200 Ma), Mesoproterozoic (1200-1500 Ma), Paleoproterozoic (1500-2200 Ma), and Archean (2200-4600 Ma). DZ U-Pb ages are plotted as kernel density estimators (KDE) and histograms, and as percentages of the 12 U-Pb components (Table 1; Figs. 4, 5).

In the eastern Jaca basin, the Belsué-Atarés deltaic and Campodarbe fluvial Formations (Bartonian-Priabonian) cropping out in the southern slopes of the External Sierras constitute the lowermost analyzed deposits (Rodellar section; Fig. 3). These formations display the highest amounts of Variscan aged zircons (> 50%, samples ROD1 and ROD3) among all the analyzed samples (Table 1; Figs. 2, 4). Upsection and to the west, the fluvial Bartonian to Priabonian Campodarbe Formation (samples BIB-1, BEMO-12 and GAL-5) records a prominent Variscan age component (20-30%), but Cambro-Devonian and Cadomian U-Pb age components increase (up to 40%) (Monrepós and Bibán sections, Fig. 4). By contrast, the uppermost parts of the late Eocene-early Miocene Campodarbe and Bernués Formations (samples ROD4, BIB5, BEMO17 and GAL10), are characterized by minor Variscan age U-Pb components (10-15%) with a dominance of Cambro-Devonian and Cadomian components (>50%), and this trend is consistent in all the sections of the eastern Jaca basin (Fig. 4). In the Luesia section (Ebro basin), the fluvial Campodarbe Formation (samples LUE9 and LUE7) shows the same evolution of the DZ-U-Pb signatures upsection. By contrast, the youngest analyzed deposits (sample LUE2, Uncastillo Formation; Ebro basin) display an important Variscan age component (up to 30%) (Fig. 4).

In the western Jaca basin (Fig. 5), the entire succession from the Ezkaba to the Bernués Formations (Bartonian to Miocene) is dominated by Cadomian and Cambro-Devonian age components (40-60%) (Yesa and Izaga sections, Fig. 3), similar to the youngest deposits of the eastern Jaca basin (Fig. 4). Therefore, the Variscan dominated to Cadomian dominated evolution of the DZ U-Pb signatures in the eastern Jaca basin is not observed in the western sector of the basin.

Multidimensional scaling and correspondence analysis (Fig. 6) allow to classify the analyzed samples into three distinct DZ U-Pb age signatures based on age populations (Figs. 6A, 6B) and age components (Figs. 6C, 6D): (i) Variscan dominated, characterized by more than 50% of Variscan age components (early Variscan + late Variscan), (ii) mixed Cadomian-Variscan, characterized by an important Variscan age component, but with higher abundances of Cadomian and Cambro-Devonian age components, and finally, (iii) Cadomian dominated, characterized by the dominance of Cadomian and Cambro-

Devonian age components (>50%) and the lowest abundance of Variscan age components.

DZ (U-Th)/He Thermochronological Signatures

DZ (U-Th)/He age populations (Table 2) are grouped into five (U-Th)/He events age: Pyrenean Orogeny (20-85 Ma), Cretaceous rifting (85-155 Ma), Liasic Cooling (180-201 Ma), Permo-Triassic Rifting (201-280 Ma), and Variscan Orogeny (280-390 Ma). Results are displayed as detrital zircon U-Pb-He double dating plots, and percentages of the five (U-Th)/He events age (Table 2; Fig. 7).

The Bartonian to Miocene clastic infill of the eastern Jaca basin (Belsué-Atarés, Campodarbe, and Bernués Formations) displays Pyrenean dominated ZHe signatures with subsidiary Cretaceous rifting and Permo-Triassic ZHe cooling ages (Fig. 7). The time equivalent deposits in the Ebro basin (samples LUE9 and LUE2 from the Luesia section) also show Pyrenean dominated ZHe signatures with subsidiary Cretaceous rifting and Permo-Triassic ZHe cooling ages, and also Variscan orogeny ages (Fig. 7). By contrast, the Bartonian to Miocene sedimentary record of the western Jaca basin is clearly represented by pre-Pyrenean dominated ZHe, with only minor Pyrenean cooling ages in some of the samples. ZHe signatures of these samples are always dominated by Permo-Triassic cooling ages, with complementary Cretaceous rifting ages and some Variscan orogeny ages. It is important to highlight that all the samples from the western Jaca basin display ZHe Liassic cooling ages, which are absent in the eastern Jaca and Ebro basins (Fig. 7).

Multidimensional scaling and correspondence analysis (Fig. 8) allow us to identify two distinct DZ ZHe signatures based on ZHe age populations (Figs. 8A, 8B) and components (Figs. 8C, 8D): (i) Pyrenean Orogeny ZHe ages dominated, characterized by more than 75% of ZHe Pyrenean ages, and (ii) pre-Pyrenean Orogeny ZHe dominated signatures, characterized by 0-15% of ZHe Pyrenean ages, major Permo-Triassic, and subsidiary Cretaceous rifting, Liasic cooling and Variscan orogeny ages.

DISCUSSION

DZ U-Pb Age Component Signatures

The Eastern Jaca Basin

A high abundance of Variscan age components is displayed in the Bartonian to Priabonian Belsué-Atarés delta and fluvial Campodarbe Formation of the southeasternmost edge of the eastern Jaca basin (Rodellar section; Fig. 6). This Variscan-dominated DZ suite can be attributed to a high contribution of Variscan granitoids and also Cretaceous sedimentary rocks containing Variscan-enriched age signatures (Hart et al. 2016; Filleaudeau et al. 2012), both sourced from the central and eastern Pyrenees through easterly-sourced axial systems (Coll et al. 2022). This is supported by the high amounts of K-feldspars and plutonic rock fragments, which are observed by sandstone petrography in these deposits (Roigé 2018; Coll et al. 2022). Upsection and to the west (Bibán, Monrepós and Gállego sections; Fig. 6), the decrease in Variscan age components and the increase of Cambro-Devonian and Cadomian age components can be linked to the drainage area reorganization that produced a shift from a plutonic-dominated towards a metamorphic-dominated source area (Michael 2013; Coll et al.

2022). Hence, we infer that the increase of sediment influx from metamorphic sources together with the decrease of granitic sources produced the shift from Variscan-dominated to mixed Cadomian-Variscan DZ U-Pb signatures. This can be linked with the Cambro-Devonian metasedimentary succession from the Pyrenees, characterized by an important Cadomian age component (Hart et al. 2016; Margalef et al. 2016), and with the Carboniferous and Triassic sedimentary rocks dominated by Cadomian and scarce Variscan age components (Hart et al. 2016; Martínez et al. 2016). The same trends both in DZ U-Pb age components (Michael 2013; Thomson et al. 2017) and petrofacies (Coll et al. 2022) are observed in the time-equivalent Escanilla Formation of the Ainsa basin, indicating that this sediment routing system (Michael, 2013) fed the eastern Jaca basin during late Eocene-Oligocene times (as also indicated by heavy mineral analysis from Coll et al., 2022).

Upsection, the uppermost Campodarbe and Bernués Formations (late Eocene-early Miocene) are characterized by Cadomian-dominated U-Pb age signatures (Fig. 6) that can be linked to the onset of sediment transport by northerly-derived transverse systems, consistent with paleocurrent orientations and sandstone petrography (Puigdefàbregas 1975; Roigé et al. 2016). The source area of these systems was mainly the Eocene turbidites of the Hecho Group, and also the Mesozoic and Paleozoic rocks from the North Pyrenean Zone (Roigé et al. 2017). The Cadomian-dominated U-Pb age signature of the north-sourced alluvial fans, which contain abundant hybrid sandstone turbidite pebbles derived from the recycling of the Hecho Group turbidites (Puigdefàbregas, 1975), contrasts with the Variscan-dominated signal that dominates most of the Hecho Group turbidites (Roigé 2018). This demonstrates the complexity of predicting DZ populations in settings with important recycling processes (Garzanti et al. 2013). Enhanced erosion of the North Pyrenean source area (Cadomian-dominated; Hart et al 2016), located at the head-waters of the drainage network of these alluvial fans (Roigé et al. 2023), or higher erosion of Cadomian-dominated Hecho Group turbidites (uppermost part) are here proposed as possible explanations for this contrasting signature between the turbidites and the alluvial fans.

The Western Jaca Basin

In the western Jaca basin (Figs. 2, 3), all the sedimentary clastic systems display monotonous DZ U-Pb Cadomian-dominated signatures (Fig. 6), similar to the north-sourced, transversely-fed systems of the eastern Jaca basin, except for the Liédena sandstone in the Izaga area, which show mixed Variscan-Cadomian signatures.

Petrographic data from the Izaga profile (Coll 2022) reveals that the Ezkaba sandstone (Bartonian), the Ardanatz (Bartonian) and the Liédena sandstone (Priabonian) Formations have a similar sandstone composition, characterized by abundant K-feldspar and fresh, unaltered plagioclase, intrabasinal bioclasts, and carbonate rock fragments that include Turonian wackestone rock fragments containing phitonellid tests. Some metamorphic and siliciclastic sandstone rock fragments, and scarce plutonic rock fragments, are also observed. This petrographic assemblage points to a source area constituted by late Cretaceous sedimentary cover and Paleozoic siliciclastic sandstones and metasediments (Coll 2022). The abundance of feldspars must be related to the recycling of Carboniferous sedimentary cover (the siliciclastic turbidites of the Culm facies) extensively outcropping in the Basque massifs, which is in accordance with Payros (1997), who inferred a siliciclastic source area located to the north, in the

Paleozoic Basque massifs for the Ezkaba sandstone (Fig. 9A). The Ezkaba, Ardanatz and Liédena Formations show DZ U-Pb Cadomian dominated signatures, which can be related to recycling of Carboniferous flysch deposits (dominated by Cadomian ages, Martinez et al. 2015), Ordovician-Devonian metasedimentary (Cambro-Devonian and Proterozoic U-Pb ages), and late Cretaceous sedimentary cover (Cadomian-dominated and mixed Variscan-Cadomian signatures), located in the North Pyrenean Zone (Hart et al. 2016).

Upsection, in the Priabonian to Chattian Campodarbe Formation (Figs. 5, 6), the same DZ U-Pb signatures and the abundance of K-feldspar and plagioclase persist (Coll 2022). Nevertheless, an important provenance change is evidenced by calcarenite rock fragments, silicified grains with idiomorphic dolomite crystals, and carbonate rock fragments, which can be related to the erosion of the sedimentary succession cropping out in the Urbasa-Andía Sierra (Payros 1997; Tariño 2006), located to the west-northwest of the study area (Fig. 9B). Therefore, in the Oligocene, the Urbasa-Andía Sierra started to deliver sediments to the Izaga area.

Finally, in the upper Izaga alluvial fan deposits, the abasence of feldspar and metamorphic grains indicates a lack of contribution from the Basque massifs, indicating that the Urbasa-Andía Sierra remained the only source (Fig. 9B). Therefore, since no U-Pb ages exist from this source area, and no shift is observed in the U-Pb DZ age signatures, sources in this area are inferred to be characterized by Cadomian dominated U-Pb signatures.

The Yesa profile also displays monotonous DZ U-Pb age signatures throughout the whole section (Figs. 5, 6). Nonetheless, the Yesa turbidites show a sandstone petrography suite with Mesozoic carbonate rock fragments (late Cretaceous mudstone-wackestone rock fragments containing phitonellid tests), K-feldspar, fresh unaltered plagioclase, and subsidiary metamorphic rock fragments, which highlight contributions from the Basque massifs and the surrounding Mesozoic sedimentary cover (Coll 2022). By contrast, Tertiary carbonate rock fragments, bioclasts and hybrid sandstone rock fragments (upper Hecho Group turbidites) point to sources located in the hanging wall of the Leyre thrust (NE).

Upsection, in the Yesa profile (Fig. 3), the Liédena sandstone shows a provenance change to Cadomian-dominated U-Pb signatures. In contrast to the Izaga area, the Liédena sandstone shows abundant metamorphic rock fragments, Permo-Triassic siliciclastic sandstone and siltstone rock fragments, crystalline carbonates, and scarce K-feldspar (Coll 2022). The similarity with the easterly-sourced Campodarbe Formation (Coll et al. 2022), and northwest-directed paleocurrents (Puigdefàbregas 1975) indicate an eastern source for this area. However, easterly-sourced systems in the eastern Jaca basin display Mixed Cadomian-Variscan U-Pb signatures. Hence, we infer that higher contributions of Permo-Triassic and metamorphic rock fragments from the eastern Pyrenees could be linked to higher amounts of Cadomian-aged zircons in the Liédena Formation (east-sourced in this area).

The overlying Campodarbe Formation shows an interplay between contributions from the Basque massifs delivering K-feldspar, fresh unaltered plagioclase and silicified rock fragments, and eastern Pyrenean sources supplying abundant metamorphic rock fragments, as well as rock fragments derived from Permo-Triassic sandstones and siltstones and crystalline limestones (Coll 2022). DZ U-Pb signatures still show

Cadomian-dominated signatures resulting from higher sediment contributions from the Basque massifs and minor supply from eastern sources. By contrast, although the top of the Campodarbe Formation still shows the same Cadomian-dominated signatures, there is no influence from eastern sources, as evidenced by the lack of metamorphic rock fragments and rock fragments from recycled Triassic sandstones, and instead records contributions from the Basque massifs and the recycling of the Eocene turbidite basin located to the north.

The Ebro Basin

In the Ebro Basin (Luesia section, Figs. 3, 5) the Campodarbe Formation shows a shift from Variscan-enriched to Variscan-impoverished DZ U-Pb signatures. This shift is the same DZ U-Pb trend recorded in the eastern Jaca basin, which corresponds to the change from east-source axially-fed systems to north-sourced transverse-fed systems (Coll et al. 2022). However, the overlying Miocene Luna fan system (Uncastillo Formation) shows a mixed Cadomian-Variscan DZ signature. The source area has been identified in the Basque massifs basement (Fig. 8B) and the earlier foreland deposits (Hecho Group and Campodarbe Formations; Hirst and Nichols 1986; Coll et al. 2022). The mixed Cadomian-Variscan U-Pb signatures of the Luna fan (Fig. 6), could be related to the recycling of the mixed Cadomian-Variscan Campodarbe and Variscan-dominated Upper Hecho Group turbidites, as evidenced by sandstone petrography detrital modes (Coll et al. 2022).

DZ ZHe Signatures

In the eastern Jaca basin (Monrepós and Gállego sections; Fig. 3), the Campodarbe Formation in the Gállego section displays ZHe signatures dominated with Pyrenean cooling ages, containing subsidiary Permo-Tiassic and Cretaceous rifting cooling age components (Figs. 7, 8). However, the Campodarbe Formation in the Monrepós section only shows Pyrenean cooling age components.

These distinct signatures must reflect to the occurrence of two different easterly-sourced axially-fed systems. This is also evidenced by distinctive heavy-mineral provenance signatures, which show one system (Monrepós section) dominated by epidote, and the other one (Gállego section) dominated by ultrastable apatite, zircon, tourmaline, and rutile (Coll et al. 2022). The Campodarbe Formation in the eastern part of the Jaca basin (Monrepós section) was fed by the fluvial Escanilla Formation (Ainsa basin), which is devoid of ZHe Permo-Triassic cooling age components (Thomson et al. 2017), and constituted one of the axially-fed systems sourced from the central Pyrenees. The other axially-fed system fed the western fluvial Campodarbe Formation (Gállego section), sourced from the eastern Pyrenees (Coll et al. 2022), where Cretaceous rifting and Permo-Triassic age cooling components are contained in the late Cretaceous-Garumnian deposits (Odlum et al. 2019). Moreover, Pyrenean ZHe cooling ages encountered in the eastern-Pyrenean sourced system are older than in the central-Pyrenean sourced system (Table 2). Therefore, ZHe provenance signatures reinforce the idea of two different sediment routing system, sourced from the central and eastern Pyrenees (Coll et al. 2022).

The youngest analyzed deposits in the Jaca basin, the north-sourced Bernués Formation, show ZHe Pyrenean dominated cooling signatures (Fig. 8), with subsidiary Cretaceous rifting and Permo-Triassic cooling age components that could be related to Cretaceous sedimentary rocks occurring in the North Pyrenean Zone, which mainly contain these DZ ZHe age signatures (i.e. the Maastrichtian; Bosch et al. 2016).

In the western Jaca basin (Izaga area), ZHe signatures are markedly different from the ones encountered in the eastern Jaca basin. The analyzed samples show ZHe pre-Pyrenean dominated cooling ages (mainly Permo-Triassic; Figs. 7, 8), pointing to the Basque massifs and Urbasa-Andía Sierra sources, which is in accordance with petrographic data (Coll 2022) and DZ U-Pb signatures. In the southern edge of the Basque massifs (Alduides massif), the Ordovician-Devonian Paleozoic basement shows ZHe signatures dominated by Cretaceous rifting cooling ages with Liasic and Permo-Triassic cooling age components (Hart et al. 2017). Therefore, the uppermost part of the present-day eroded Paleozoic basement (mainly Carboniferous) must have sourced zircon grains from shallow crustal depths above the partial retention zone, with cooling ages older than Pyrenean orogenesis, like the ones sourced from the Ebro Massif and contained in the late Cretaceous siliciclastic formations (Filleaudeau et al 2012, Odlum et al 2019). The increase of sediment recycling towards the uppermost part of the Izaga section, evidenced by the higher proportions of sandstone rock fragments (Coll 2022), does not have an impact on the distribution of the ZHe cooling ages which remain constant through all the section (Fig. 7).

Finally, the Uncastillo Formation in the Ebro basin (Luesia section; Fig. 2) displays Pyrenean-dominated ZHe ages (Figs. 7, 8) with subordinate Permo-Triassic and Variscan ZHe cooling age components. Since this alluvial fan records the erosion of the Hecho Group turbidites, the Jaca thrust sheet top basin, and the Basque massifs (Hirst and Nichols 1986; Coll et al. 2022), ZHe Pyrenean cooling ages must be linked to the recycling of earlier foreland basin deposits (Hecho Group and Campodarbe Formations) containing Pyrenean ZHe cooling ages, whereas Permo-Triassic and Variscan cooling age components must be linked to the Paleozoic and Mesozoic sedimentary cover occurring in the Basque massifs and NPZ.

Therefore, the dominance of pre-Pyrenean or Pyrenean ZHe cooling ages in the Jaca basin deposits is linked to the contribution of two source area domains with a clear differentiated exhumational history (i.e. the Basque Massifs and the Pyrenees) rather than the evolution of a single source area.

Synthesis of the South Pyrenean Sediment Routing Systems

The Eastern Jaca Basin

During late Lutetian to Bartonian times, deltaic sedimentation in the southern Jaca basin (Fig. 9) was mainly derived from eastern source areas through a unique fluvial system during the first sedimentation stage (Coll et al. 2022). These sources were the Paleozoic basement (mostly Variscan granitoids) and the Mesozoic and Paleogene sedimentary cover of the growing central Pyrenees. In the northern Jaca basin, deltaic sedimentation was represented by the Sabiñánigo delta, which records the initial erosion of the west-central Pyrenes (Roigé et al. 2016).

From early Priabonian onwards, two distinct axially-fed fluvial systems from the central and eastern Pyrenees respectively, one dominated by epidote, and the other characterized by the absence of epidote and subsidiary Cretaceous rifting and Permo-Triassic ZHe cooling ages, were delivering sediment to the basin (see Coll et al. 2022 for heavy mineral contents). Both systems were sourced from Variscan granitoids and a

Mesozoic sedimentary cover, and evolved, during the Priabonian, to a more dominant metamorphic composition during the Priabonian persisting until Chattian times (Coll et al. 2022). ZHe Pyrenean signatures dominate both of these systems (Fig. 7).

The youngest deposits of the Jaca basin (uppermost Campodarbe and Bernués Formations), record the recycling of the uppermost sedimentary systems of the former Eocene turbidite basin (Fig. 9) with contributions from the North Pyrenean Zone (Roigé et al. 2017; Coll et al. 2022).

The Western Jaca Basin

In the Bartonian, the Ezkaba channel-levee complex records the first input of northerly-derived systems sourced from the Basque massifs (Payros et al. 1997), mainly from Carboniferous Culm facies with contributions from a Cretaceous sedimentary cover (Fig. 9). The overlying Ardanatz delta still registers the Basque massifs as an active source, which extended its influence to the west during the sedimentation of the Priabonian Yesa turbidites. However, during the last stages of the Priabonian sedimentation (Liédena sandstone), a strong interplay between Western and Eastern Pyrenean, as well as west-central Pyrenean sources occurred in the limit between the eastern and western Jaca basin.

During the deposition of the middle Campodarbe Formation (Rupelian), eastern and western Pyrenean sources influenced the sedimentation in the Yesa area, whereas the Izaga area started to receive contributions from the Urbasa-Andía Sierra. In the Chattian-Aquitanian, whereas the Yesa area was fed from the west, west-central, central-eastern

Pyrenean sources, the Urbasa-Andía sources dominated in the Izaga area and contributions from the Basque massifs stopped in this part of the basin (Fig. 9).

The Ebro Basin

During Priabonian-Rupelian times, the lower Campodarbe Formation in the Ebro basin was fed from eastern Pyrenean sources, which are the same source areas as the time-equivalent deposits in the present-day Gállego Valley (eastern Jaca basin). Northerly-sourced systems, which during the Eocene were restricted to the Jaca basin, reached the Ebro basin during Chattian. Finally, the Aquitanian Luna alluvial fan system was sourced from the erosion of the Eocene turbidite basin, the wedge top Jaca basin, and the Basque massifs (Roigé et al. 2019) (Fig. 9).

Insights into the Propagation of DZ U-Pb Age Signatures

The main controlling factors influencing the DZ geochronologic and thermochronologic signatures in clastic successions are source rock age distributions, source rock zircon fertility, lithologic erodibility, signal modulation by sediment transport and the relative contribution of each lithology to the analyzed grain-size window (e.g. Malusà et al. 2016; Capaldi et al. 2017; Jackson et al. 2019). DZ U-Pb age signatures of potential sources and zircon fertility should be obtained from the analysis of each lithology in the source areas, and the relative contribution of source areas can only be inferred from detailed sandstone petrography. In our work, source rock age distributions and zircon fertility have been described in section 2.2, and detailed sandstone petrography from Coll et al. (2022) has been used to assess the relative contribution of each lithology.

In the southern margin of the Jaca basin, sedimentary systems with a high granitic component (Belsué-Atarés, Rodellar section) display U-Pb Variscan dominated signatures, which do not change in the overlying systems of the Campodarbe Formation that were influenced by a metamorphic source area with a scarce granitic component (Coll et al. 2022). Further west, the Belsué-Atarés Formation in the Monrepós section is characterized by mixed Cadomian-Variscan U-Pb age signatures, which also do not change in the overlying systems (Campodarbe Formation). In both situations, the fact that no correlation exists between the abundance of granitic rock fragments and Variscan U-Pb age components imply a non-granitic lithology in the source area that provided enough Variscan zircons to offset the persistence of the other U-Pb signatures. Therefore, we infer the Cretaceous sedimentary cover as an important contributor of Variscan zircons, which can be characterized by U-Pb Variscan-dominated signatures (Filleaudeau et al., 2012; Odlum et al., 2019). The contribution of this source is supported by the presence of carbonate rock fragments observed in both petrofacies, and highlights that recycling of sedimentary cover rocks can contribute to the propagation of Variscan DZ age components. This demonstrates that provenance analysis solely based on U-Pb ages without considering the role of recycling in the propagation of U-Pb age signatures might lead to misinterpretations regarding the nature of the source areas in foreland basins (e.g. Jackson et al. 2019, Schwartz et al. 2019).

The recycling of the Hecho Group turbidites of the northern Jaca basin, characterized by Variscan-dominated (Banastón and lower Jaca turbidite systems) to Cadomian-dominated (middle-upper Jaca turbidite systems) signatures (Roigé 2018) should propagate, at least, mixed Cadomian-Variscan signatures due to their high abundance in the sand fraction (Coll et al. 2022). However, the alluvial fans recycling the Hecho Group turbidites (hybrid clast-dominated north-sourced systems) display Cadomian-dominated signatures. Even if inferring low zircon fertility for the Hecho Group turbidites source (although moderate-high fertility is expected according to Roigé et al. 2023), their higher contribution in front of Paleozoic metasedimentary and siliciclastic sandstone sources (Cadomian-dominated age signatures) would be enough to produce mixed Cadomian-Variscan signatures. Even if we assume that the second most represented source in the north-sourced systems (the Cretaceous sedimentary cover) delivered Cadomian-dominated signatures (Hart et al. 2016), the representation of these rocks in the source area would not be volumetrically enough to mask Variscan-enriched signatures, as evidenced by the limited proportions of Mesozoic rocks fragments in the alluvial fans (Roigé et al. 2017). Therefore, DZ U-Pb highlights Cadomian-dominated signatures derived from major recycling of the turbidite basin is linked to main contributions to the middle-upper Jaca turbidite systems.

Conversely, in the western Jaca basin, monotonous DZ U-Pb Cadomian-dominated signatures are displayed in all the analyzed deposits. This contrasts with the several compositional changes recorded by sandstone petrography in these deposits. Therefore, we can infer that DZ U-Pb fails to discriminate between the different source areas. However, U-Pb provenance signatures highlight the recycling of the Carboniferous sedimentary cover. K-feldspar, plagioclase and subsidiary plutonic rock fragments might indicate a granitic source that could be related to Ordovician gneisses or Variscan granitoids from the Paleozoic basement of the Basque massifs. However, in this case, the high contribution from these crystalline sources together with high zircon fertility would strongly increase Cambro-Devonian (gneiss) or Variscan age signatures (granites). Nevertheless, since Variscan or Cambro-Devonian dominated signatures are not observed, DZ U-Pb indicates recycling of detrital Carboniferous zircons instead of a direct granitic/gneissic source. Late Variscan ages would be derived from Cretaceous and Paleocene-Eocene sediments also present in the source areas. In conclusion, DZ U-Pb in the western Jaca basin highlights the role of recycled versus direct sources.

Finally, in the Ebro basin, provenance constraints from sandstone petrography allow a better understanding of DZ U-Pb signature propagation. The Miocene Luna alluvial fan (Fig. 8B) system is sourced from the Basque massifs and the recycling of the Hecho Group turbidites and Campodarbe Formation (Hirst and Nichols 1986; Arenas 1993, Roigé et al. 2019). In this case, the mixed Cadomian-Variscan signatures reflect contributions from the Campodarbe Formation, as well as from the Variscan-dominated Banastón and lower Jaca turbidite systems. The onset of Miocene sedimentation in the Ebro basin probably was accompanied by a major incision on these formations in the hinterland, increasing contributions from this source and leading to an increase in Variscan age components in the Luna alluvial fan.

Summarizing, in the western Jaca basin provenance analysis solely based on DZ U-Pb has failed to highlight the interplay between western Pyrenean, eastern Pyrenean, and west-central Pyrenean sources (Fig. 6), as well as to discriminate recycled versus first cycle sources. In the Pyrenees, DZ U-Pb signatures stand as a good proxy to distinguish between Variscan granites, Ordovician gneiss, Cambro-Devonian metasedimentary, and Carboniferous to Permo-Triassic sources due to their well-known provenance signatures. However, when Cretaceous, Paleocene and Eocene contributions are underrepresented, to unequivocally unravel provenance may become unrealistic. Although integration with DZ ZHe signatures can aid to reduce the ambiguity of provenance signals, a good control of the source area lithology contribution based on sandstone detrital modes is necessary to fully understand how DZ age signatures are propagated and to avoid biased provenance inferences. So, DZ age signatures highly increase their power as a reliable provenance indicator when coupled with petrographic data. Therefore, studies combining sandstone petrography, U-Pb, and ZHe provenance signatures stand as the most powerful tool to obtain the highest resolution in sedimentary provenance analysis while interpretations based solely on single-method approaches must be taken with caution.

CONCLUSIONS

The integration of the three distinct DZ U-Pb signatures (Variscan-dominated, mixed Cadomian-Variscan, and Cadomian-dominated) and two ZHe cooling signatures (Pyrenean-dominated, and pre-Pyrenean dominated) defined in this work, combined with sandstone petrography, allowed to characterize different routing systems with distinct source areas in the Jaca basin of the South Pyrenean foreland.

DZ U-Pb and (U-Th)/He data of Bartonian to Miocene deltaic to fluvial-alluvial deposits indicate that the eastern and western Jaca basins have different provenance signatures. While the eastern Jaca basin was sourced from the central and eastern Pyrenees to the east of the basin, and recorded the evolution of these source areas until the onset of north-derived systems recycling an earlier turbidite foredeep, the western Jaca basin was mainly sourced by the western Pyrenees (Basque massifs and the thrust units of the Urbasa-Andía Sierra).

Our work demonstrates that the western sources extended their influence to the Yesa area through the Ardanatz, Yesa turbidites and Campodarbe Formations, which is in contrast with previous interpretations that linked these systems to the progradation of the Belsué-Atarés delta system of the eastern Jaca basin. Moreover, our data highlights the interplay between different zones of the Pyrenean domain in the Yesa area during the sedimentation of the fluvial Campodarbe Formation, which also contradicts the classical view of an east-sourced fluvial system transferring sediment to the western Jaca basin.

Coupling DZ U-Pb, (U-Th)/He and sandstone petrography allow to understand the propagation of DZ signatures and to identify the role of direct vs recycled sources. Our results indicate that zircon U-Pb signatures are more likely to reflect recycled sources than first-cycle sources. On the other hand, complementing petrographic data with DZ signatures permits to highlight the contributions from specific sources such as the uppermost Hecho Group turbidites of the Eocene, recycled foreland basin or the Carboniferous cover of the Basque massifs. Our work highlights the power of coupling sandstone petrography with DZ geochronology and thermochronology to constrain sediment sources and avoid biased provenance interpretations in foreland basins fed from recycling sedimentary rocks in growing orogens.

ACKNOWLEDGMENTS

This work is a contribution to the projects PID2021-122467NC-C21 and PGC2018-B-C21, financed by the MCIU of Spain. The authors are very grateful for support from the Jackson School of Geosciences (UT). We thank Lisa Gilley Stockli and UTChron lab staff for assistance during the detrital zircon U-Pb analysis and for fruitful discussions. We are very grateful to Kelly Thomson, Thomas Capaldi and the Editor Kathleen M Marsaglia for their constructive reviews that greatly helped to improve the manuscript.

REFERENCES

Allen, P. A., 2017, Sediment routing systems: The fate of sediment from source to sink: Cambridge University Press, Cambridge, 407p.

Andò, S., 2020, Gravimetric separation of heavy minerals in sediments and rocks: *Minerals*, v. 10, p. 273.

Arenas, C., 1993, Sedimentología y paleogeografía del Terciario del margen pirenaico y sector central de la Cuenca del Ebro (zona aragonesa occidental) (PhD tesis): Universidad de Zaragoza, Zaragoza, Spain, 858p.

Arenas, C., Millán, H., Pardo, G., and Pocoví, A., 2001, Ebro Basin continental sedimentation associated with late compressional Pyrenean tectonics (north-eastern Iberia): controls on basin margin fans and fluvial systems: Basin Research, v. 13, p. 65-89.

Astibia, H., Elorza, J., Pisera, A., Alvarez-Pérez, G., Payros, A., and Ortiz, S., 2014, Sponges and corals from the Middle Eocene (Bartonian) marly formations of the Pamplona Basin

(Navarre, Western Pyrenees): taphonomy, taxonomy, and paleoenvironments: Facies, v. 60, p. 91-110.

Astibia, H., Payros, A., Suberbiola, X. P., Elorza, J., Berreteaga, A., Etxebarria, N., Badiola, A., and Tosquella, J., 2005, Sedimentology and taphonomy of sirenian remains from the Middle Eocene of the Pamplona Basin (Navarre, western Pyrenees): Facies, v. 50, p. 463-475.

Barnolas, A., and Gil-Peña, I., 2001, Ejemplos de relleno sedimentario multiepisódico en una cuenca de antepaís fragmentada: La Cuenca Surpirenaica: Boletín Geológico y Minero, v. 112, p. 17-38.

Barnolas, A., and Teixell, A., 1994, Platform sedimentation and collapse in a carbonate-dominated margin of a foreland basin (Jaca basin, Eocene, southern Pyrenees): Geology, v. 22, p. 1107-1110.

Bentham, P. A., Burbank, D. W., and Puigdefabregas, C., 1992, Temporal and spatial controls on the alluvial architecture of an axial drainage system: late Eocene Escanilla Formation, southern Pyrenean foreland basin, Spain: Basin Research, v. 4, p. 335-352.

Bernard, T., Sinclair, H. D., Gailleton, B., Mudd, S. M., and Ford, M., 2019, Lithological control on the post-orogenic topography and erosion history of the Pyrenees. Earth and Planetary Science Letters, v. 518, p. 53-66.

Bosch, G. V., Teixell, A., Jolivet, M., Labaume, P., STockli, D., Domenech, M., and Monie, P., 2016, Timing of Eocene–Miocene thrust activity in the Western Axial Zone and

Chaînons Béarnais (west-central Pyrenees) revealed by multi-method thermochronology: Comptes Rendus Géoscience, v. 348, p. 246-256

Boya, S., 2018. El sistema deltaico de la Arenisca de Sabiñánigo y la continentalización de la cuenca de Jaca (PhD tesis): Universitat Autònoma de Barcelona, Bellaterra, Spain, 231p.

Burrel, L., and Teixell, A., 2021, Contractional salt tectonics and role of pre-existing diapiric structures in the Southern Pyrenean foreland fold–thrust belt (Montsec and Serres Marginals): Journal of the Geological Society, v. 178, jgs2020-085.

Burrel, L., Teixell, A., Gómez-Gras, D., and Coll, X., 2021, Basement-involved thrusting, salt migration and intramontane conglomerates: a case from the Southern Pyrenees: BSGF-Earth Sciences Bulletin, v. 192, p 24.

Caja, M.A., Marfil, R., Garcia, D., Remacha, E., Morad, S., Mansurbeg, H., Amorosi, A., Martínez-Calvo, C. and Lahoz-Beltrá, R., 2010, Provenance of siliciclastic and hybrid turbiditic arenites of the Eocene Hecho Group, Spanish Pyrenees: implications for the tectonic evolution of a foreland basin: Basin Research, v. 22, p. 157-180.

Cámara, P., and Klimowitz, J., 1985, Interpretación geodinámica de la vertiente centro-occidental surpirenaica (Cuencas de Jaca-Tremp): Estudios geológicos, v. 41, p. 391-404.

Campbell, I. H., Reiners, P. W., Allen, C. M., Nicolescu, S., and Upadhyay, R., 2005, He–Pb double dating of detrital zircons from the Ganges and Indus Rivers: Implication for quantifying sediment recycling and provenance studies: Earth and Planetary Science Letters, v. 237, p. 402-432.

Capaldi, T.N., Horton, B.K., McKenzie, N.R., STockli, D.F. and Odlum, M.L., 2017, Sediment provenance in contractional orogens: The detrital zircon record from modern rivers in the Andean fold-thrust belt and foreland basin of western Argentina. Earth and Planetary Science Letters, v. 479, p. 83-97.

Capaldi, T. N., Odlum, M. L., Curry, M. E., and Stockli, D. F., 2022, Variable thermal histories across the Pyrenees orogen recorded in modern river sand detrital geo-/ thermochronology and PECUBE thermokinematic modelling. Basin Research, V. 00, 1–26.

Coll, X., 2022, Procedència i patró de dispersió de sediments en conques d'avantpaís: Avantatges d'un enfoc mulimètode i aplicación al cas de la conca sudpirinenca de Jaca. PhD tesis: Universitat Autònoma de Barcelona, Bellaterra, Spain, 308pp.

Coll, X., Gómez-Gras, D., Roigé, M., Teixell, A., Boya, S., and Mestres, N., 2020, Heavy-mineral provenance signatures during the infill and uplift of a foreland basin: An example from the Jaca basin (southern Pyrenees, Spain): Journal of Sedimentary Research, v. 90, p. 1747-1769.

Coll, X., Roigé, M., Gómez-Gras, D., Teixell, A., Boya, S., and Mestres, N., 2022, Interplay of Multiple Sediment Routing Systems Revealed by Combined Sandstone Petrography and Heavy Mineral Analysis (HMA) in the South Pyrenean Foreland Basin: Minerals, v. 12, p. 1-29.

Costa, E., Garces, M., López-Blanco, M., Beamud, E., Gómez-Paccard, M., and Larrasoaña, J. C., 2010, Closing and continentalization of the South Pyrenean foreland basin (NE Spain): magnetochronological constraints: Basin Research, v. 22, p. 904-917.

Denele, Y., Barbey, P., Deloule, E., Pelleter, E., Olivier, P., and Gleizes, G., 2009, Middle Ordovician U-Pb age of the Aston and Hospitalet orthogneissic laccoliths: their role in the Variscan evolution of the Pyrenees: Bulletin de la Société géologique de France, v. 180, p. 209-216.

Dickinson, W. R., 1970, Interpreting detrital modes of graywacke and arkose. Journal of Sedimentary Research, v. 40, p. 695-707.

Dickinson, W. R., 2008, Impact of differential zircon fertility of granitoid basement rocks in North America on age populations of detrital zircons and implications for granite petrogenesis: Earth and Planetary Science Letters, v. 275, p. 80-92.

Dickinson, W. R., and Gehrels, G. E., 2009, Use of U–Pb ages of detrital zircons to infer maximum depositional ages of strata: a test against a Colorado Plateau Mesozoic database: Earth and Planetary Science Letters, v. 288, p. 115-125.

Dickinson, W. R., and Suczek, C. A., 1979, Plate tectonics and sandstone compositions: AAPG Bulletin, v. 63, p. 2164-2182.

Dreyer, T., Corregidor, J., Arbues, P., and Puigdefabregas, C., 1999, Architecture of the tectonically influenced Sobrarbe deltaic complex in the Ainsa Basin, northern Spain: Sedimentary Geology, v. 127, p. 127-169.

Farley, K. A., Wolf, R. A., and Silver, L. T., 1996, The effects of long alpha-stopping distances on (U-Th)/He ages. Geochimica et Cosmochimica Acta, v. 60, 4223-4229.

Farley, K. A., 2002, (U-Th)/He dating: Techniques, calibrations, and applications. Reviews in Mineralogy and Geochemistry, v. 47, p. 819-844.

Filleaudeau, P. Y., Mouthereau, F., and Pik, R., 2012, Thermo-tectonic evolution of the south-central Pyrenees from rifting to orogeny: Insights from detrital zircon U/Pb and (U-Th)/He thermochronometry: Basin Research, v. 24, p. 401-417.

Fontana, D., Zuffa, G. G., and Garzanti, E, 1989, The interaction of eustacy and tectonism from provenance studies of the Eocene Hecho Group Turbidite Complex (South-Central Pyrenees, Spain): Basin Research, v. 2, p. 223-237.

Fosdick, J. C., Grove, M., Graham, S. A., Hourigan, J. K., Lovera, O., and Romans, B. W., 2015, Detrital thermochronologic record of burial heating and sediment recycling in the Magallanes foreland basin, Patagonian Andes: Basin Research, v. 27, p. 546-572.

Garzanti, E., and Andò, S., 2019, Heavy minerals for junior woodchucks: Minerals, v. 9, p. 148.

Garzanti, E., Andò, S., and Vezzoli, G., 2008, Settling equivalence of detrital minerals and grain-size dependence of sediment composition: Earth and Planetary Science Letters, v. 273, p. 138-151.

Garzanti, E., Andò, S., and Vezzoli, G., 2009, Grain-size dependence of sediment composition and environmental bias in provenance studies: Earth and Planetary Science Letters, v. 277, p. 422-432.

Garzanti, E., Doglioni, C., Vezzoli, G., and Ando, S., 2007, Orogenic belts and orogenic sediment provenance: The Journal of Geology, v. 115, p. 315-334.

Garzanti, E., Limonta, M., Resentini, A., Bandopadhyay, P. C., Najman, Y., Andò, S., and Vezzoli, G., 2013, Sediment recycling at convergent plate margins (Indo-Burman ranges and Andaman–Nicobar Ridge): Earth-Science Reviews, v. 123, p. 113-132.

Garzanti, E., Vezzoli, G., Lombardo, B., Ando, S., Mauri, E., Monguzzi, S., and Russo, M., 2004, Collision-orogen provenance (western Alps): Detrital signatures and unroofing trends: The Journal of Geology, v. 112, p. 145-164.

Gómez-gras, D., Roigé, M., Fondevilla, V., Oms, O., Boya, S., and Remacha, E., 2016, Provenance constraints on the Tremp Formation paleogeography (southern Pyrenees): Ebro Massif vs Pyrenees sources: Cretaceous Research, v. 57, p. 414-427.

Gupta, K. D., and Pickering, K. T., 2008, Petrography and temporal changes in petrofacies of deep-marine Ainsa–Jaca basin sandstone systems, Early and Middle Eocene, Spanish Pyrenees: Sedimentology, v. 55, p. 1083-1114.

Hart, N. R., 2015, Temporal constraints on progressive rifting of a hyper-extended continental margin using bedrock and detrital zircon (U-Th)/(Pb-He) dating, Mauléon Basin, western Pyrenees (PhD thesis): University of Texas at Austin, Austin (USA).

Hart, N. R., Stockli, D. F., and Hayman, N. W., 2016, Provenance evolution during progressive rifting and hyperextension using bedrock and detrital zircon U-Pb geochronology, Mauléon Basin, western Pyrenees: Geosphere, v. 12, p. 1166-1186.

Hart, N. R., Stockli, D. F., LAvier, L. L., and Hayman, N. W., 2017, Thermal evolution of a hyperextended rift basin, Mauléon Basin, western Pyrenees: Tectonics, v. 36, p. 1103-1128.

Hirst, J. P. P., and Nichols, G. J., 1986, Thrust tectonic controls on Miocene alluvial distribution patterns, southern Pyrenees: Foreland basins, p. 247-258.

Hogan, P. J., 1993, Geochronologic, tectonic and stratigraphic evolution of the Southwest Pyrenean foreland basin, northern Spain (Phd thesis). University of southern California, Los Ángeles, USA, 208p.

Hogan, P. J., and Burbank, D. W. 1996, Evolution of the Jaca piggyback basin and emergence of the External Sierra, southern Pyrenees, in Friend, P., and Dabrio, C., eds., Tertiary Basins of Spain: Cambridge, Cambridge University Press, p. 153–160.

Hudec, M. R., Dooley, T. P., Burrel, L., Teixell, A., and Fernandez, N., 2021, An alternative model for the role of salt depositional configuration and preexisting salt structures in the evolution of the Southern Pyrenees, Spain: Journal of Structural Geology, v. 146, p. 104-325.

Jackson, S. E., Pearson, N. J., Griffin, W. L., and Belousova, E. A., 2004, The application of laser ablation-inductively coupled plasma-mass spectrometry to in situ U–Pb zircon geochronology: Chemical Geology, v. 211, p. 47-69.

Jackson, L.J., Horton, B.K., and Vallejo, C., 2019, Detrital zircon U-Pb geochronology of modern Andean rivers in Ecuador: Fingerprinting tectonic provinces and assessing downstream propagation of provenance signals: Geosphere v. 15, p. 1943–1957, doi: 10.1130/GES02126.1.

Jolley, E. J., 1987, Thrust tectonics and alluvial architecture of the Jaca Basin, Southern Pyrenees (PhD thesis): University of Walles, Cardiff, UK, 365 pp.

Koshnaw, R. I., Stockli, D. F., and Schlunegger, F., 2019, Timing of the Arabia-Eurasia continental collision—Evidence from detrital zircon U-Pb geochronology of the Red Bed Series strata of the northwest Zagros hinterland, Kurdistan region of Iraq: Geology, v. 47, p. 47-50.

Labaume, P., Meresse, F., Jolivet, M., Teixell, A., and Lahfid, A., 2016, Tectono-thermal history of an exhumed thrust-sheet-top basin: An example from the south Pyrenean thrust belt: Tectonics, v. 35, p. 1280-1313.

Labaume, P., Séguret, M., and Seyve, C., 1985, Evolution of a turbiditic foreland basin and analogy with an accretionary prism: Example of the Eocene south-Pyrenean basin: Tectonics, v. 4, p. 661-685.

Labaume, P., and Teixell, A., 2018, 3D structure of subsurface thrusts in the eastern Jaca Basin, southern Pyrenees: Geologica Acta, p. 477-498.

Lagabrielle, Y., Labaume, P., and De Saint Blanquat, M., 2010, Mantle exhumation, crustal denudation, and gravity tectonics during Cretaceous rifting in the Pyrenean realm (SW Europe): Insights from the geological setting of the lherzolite bodies: Tectonics, v. 29, p. 1-26.

Laskari, S., Soukis, K., Lozios, S., Stockli, D. F., Poulaki, E. M., and Stouraiti, C., 2021, Provenance Analysis and Structural Study of the Cycladic Blueschist Unit Rocks from Iraklia Island: From the Paleozoic Basement Unroofing to the Cenozoic Exhumation: Minerals, v. 12, p. 83

Laskari, S., Soukis, K., Stockli, D. F., Lozios, S., and Zambetakis-Lekkas, A., 2022, Reconstructing the southern Pelagonian domain in the Aegean Sea: Insights from U-Pb detrital zircon analysis, lithostratigraphic and structural study, and zircon (U-Th)/He thermochronology on Amorgos Island (SE Cyclades, Greece): Gondwana Research, v. 106, p. 329-350.

Lescoutre, R., and Manatschal, G., 2020, Role of rift-inheritance and segmentation for orogenic evolution: example from the Pyrenean-Cantabrian system, BSGF - Earth Sciences Bulletin, v. 191, 18.

Malusà, M. G., Resentini, A., and Garzanti, E., 2016, Hydraulic sorting and mineral fertility bias in detrital geochronology: Gondwana Research, v. 31, p. 1-19.

Mangin, J.P., 1960. Le Nummulitique Sud-Pyrénéen à l'ouest de l'Aragón: Pirineos, v. 58, 79–83.

Margalef, A., Castiñeiras, P., Casas, J.M., Navidad, M., Liesa, M., Linnemann, U., Hofmann, M., and Gärtner, A., 2016, Detrital zircons from the Ordovician rocks of the Pyrenees: Geochronological constraints and provenance: Tectonophysics, v. 681, p. 124-134.

Martí, J., Mitjavila, J., Roca, E., and Aparicio, A., 1992, Cenozoic magmatism of the Valencia trough (western Mediterranean): Relationship between structural evolution and volcanism: Tectonophysics, v. 203, p. 145-165.

Martínez, F.J., Iriondo, A., Dietsch, C., Aleinikoff, J.N., Peucat, J.J., Cirès, J., Reche, J. and Capdevila, R., 2011, U-Pb SHRIMP-RG zircon ages and Nd signature of lower Paleozoic rifting-related magmatism in the Variscan basement of the Eastern Pyrenees: Lithos, v. 127, p. 10-23.

Martínez, F. J., Reche, J., and Iriondo, A., 2008, U–Pb Shrimp-RG zircon ages of Variscan igneous rocks from the Guilleries massif (NE Iberia pre-Mesozoic basement). Geological implications: Comptes Rendus Geoscience, v. 340, p. 223-232.

Marzoli, A., Renne, P. R., Piccirillo, E. M., Ernesto, M., Bellieni, G., and Min, A. D., 1999, Extensive 200-million-year-old continental flood basalts of the Central Atlantic Magmatic Province: Science, v. 284, p. 616-618.

Michael, N., 2013, Functioning of an ancient routing system, the Escanilla Formation, South Central Pyrenees (PhD thesis): Imperial College London, London, UK, 284 p.

Moecher, D. P., and Samson, S. D., 2006, Differential zircon fertility of source terranes and natural bias in the detrital zircon record: Implications for sedimentary provenance analysis: Earth and Planetary Science Letters, v. 247, p. 252-266.

Mouthereau, F., Filleaudeau, P. Y., Vacherat, A., Pik, R., Lacombe, O., Fellin, M.G., Castelltort, S., Christophoul, F., and Masini, E., 2014, Placing limits to shortening evolution in the Pyrenees: Role of margin architecture and implications for the Iberia/Europe convergence: Tectonics, v. 33, p. 2283-2314.

Muñoz, J. A., Mencos, J., Roca, E., Carrera, N., Gratacós, O., Ferrer, O., and Fernández, Ò., 2018, The structure of the South-Central-Pyrenean fold and thrust belt as constrained by subsurface data: Geologica Acta, p. 439-460.

Mutti, E., 1985, Turbidite systems and their relations to depositional sequences. In Provenance of arenites. Springer, Dordrecht, p. 65-93.

Mutti, E., Luterbacher, H., Ferrer, J., and Rosell, J., 1972, Schema stratigrafico e lineamenti di facies del Paleogeno Marino della zona centrale sudpirenaica tra Tremp (Catalogna) e Pamplona (Navarra): Mem. Soc. Geol. Ital. v. 11, p. 391–416.

Nijman, W., and Nio, S., 1975, The Eocene Montañana Delta (Tremp–Graus Basin, provinces of Lérida and Huesca, Southern Pyrenees, N Spain), Field Trip B Guidebook. The Sedimentary Evolution of the Paleogene South Pyrenean Basin): International Association of Sedimentologists, XI International Sedimentological Congress, Excursion Guidebook, p. 1–20.

Odlum, M. L., Stockli, D. F., Capaldi, T. N., Thomson, K. D., Clark, J., Puigdefàbregas, C., and Fildani, A., 2019, Tectonic and sediment provenance evolution of the South Eastern Pyrenean foreland basins during rift margin inversion and orogenic uplift: Tectonophysics, v. 765, p. 226-248.

Oliva-Urcia, B., Beamud, E., Arenas, C., Pueyo, E. L., Garcés, M., Soto, R., Valero, L., and Pérez-Rivarés, F. J., 2019, Dating the northern deposits of the Ebro foreland basin; implications for the kinematics of the SW Pyrenean front: Tectonophysics, v. 765, p. 11-34.

Oliva-Urcia, B., Beamud, E., Garcés, M., Arenas, C., Soto, R., Pueyo, E. L., and Pardo, G., 2016, New magnetostratigraphic dating of the Palaeogene syntectonic sediments of the west-central Pyrenees: tectonostratigraphic implications: Geological Society, London, Special Publications, v. 425, p. 107-128.

Oms, O., Dinarès-Turell, J., and Remacha, E., 2003, Magnetic stratigraphy from deep clastic turbidites: an example from the Eocene Hecho group (southern Pyrenees): Studia Geophysica et Geodaetica, v. 47, p. 275-288.

Ortí, F., Salvany, J.M., RoselL, L., Pueyo, J.J., and Inglés, M., 1986, Evaporitas antiguas (Navarra) y actuales (Los Monegros) de la Cuenca del Ebro, in Anadón, P., and Cabrera, L., eds., Guía de Las Excursiones Del XI Congreso Español de Sedimentologia: Generalitat de Catalunya, Comissió Interdepartamental de Recerca i Innovació Tecnològica, Barcelona, p. 21–21.

Paton, C., Hellstrom, J., Paul, B., Woodhead, J., and Hergt, J., 2011, Iolite: Freeware for the visualisation and processing of mass spectrometric data. Journal of Analytical Atomic Spectrometry, v. 26, p. 2508-2518.

Payros, A., Astibia, H., Cearreta, A., Pereda-Suberbiola, X., Murelaga, X., and Badiola, A., 2000, The Upper Eocene South Pyrenean Coastal deposits (Liedena sandstone, navarre): Sedimentary facies, benthic formanifera and avian ichnology: Facies, v. 42, p. 107-131.

Payros, A., Pujalte, V., Orue-Etxebarria, X., and Baceta, J. I., 1997, A Bartonian channel-levee turbiditic system in the Pamplona Basin: Tectonic and paleogeographic implications: Geogaceta, v. 22, p. 145-148.

Payros, A., Pujalte, V., and Orue-Etxebarria, X., 1999, The South Pyrenean Eocene carbonate megabreccias revisited: new interpretation based on evidence from the Pamplona Basin: Sedimentary Geology, v. 125, p. 165-194.

Puigdefàbregas, C., 1975, La sedimentación molásica en la cuenca de Jaca: Pirineos, v. 104, p. 1–188.

Puigdefàbregas, C., Muñoz, J. A., and Vergés, J., 1992, Thrusting and foreland basin evolution in the southern Pyrenees. In Thrust tectonics (pp. 247-254). Springer, Dordrecht.

Pujols, E. J., and Stockli, D. F., 2021, Zircon (U-Th)/(He-Pb) double-dating constraints on the interplay between thrust deformation and foreland basin architecture, Sevier foreland basin, Utah. Geosphere, v. 17, p. 1890-1913.

Rat, J., Mouthereau, F., Brichau, S., Vacherat, A., Fillon, C. and Gautheron, C., 2022, Timing and distribution of exhumation in the Ebro basin reveal a plate-scale 10 Ma geodynamic event. Global and Planetary Change, V. 218, p. 103973.

Reiners, P. W., 2005, Zircon (U-Th)/He thermochronometry: Reviews in Mineralogy and Geochemistry, v. 58, p. 151-179.

Remacha, E., Fernández, L. P., and Maestro, E., 2005, The transition between sheet-like lobe and basin-plain turbidites in the Hecho Basin (South-Central Pyrenees, Spain): Journal of Sedimentary Research, v. 75, p. 798-819.

Roigé M., 2018, Procedència i evolució dels sistemes sedimentaris de la conca de Jaca (conca d'avantpaís Sudpirinenca): Interacció entre diverses àrees font en un context tectònic actiu (PhD thesis)., Universitat Autònoma de Barcelona, Bellaterra, Spain, 312p.

Roigé, M., Gómez-Gras, D., Stockli, D. F., Teixell, A., Boya, S., and Poyatos-Moré, M., 2023. Recycling effects in detrital zircon UPb signatures in a foreland basin: Identifying the multicyclic sediment sources of the Eocene-Miocene Jaca basin (southern Pyrenees, Spain). Sedimentary Geology, 456, 106500.

Roigé, M., Gómez-Gras, D., Remacha, E., Boya, S., Viaplana-Muzas, M., and Teixell, A., 2017, Recycling an uplifted early foreland basin fill: An example from the Jaca basin (Southern Pyrenees, Spain): Sedimentary Geology, v. 360, p. 1-21.

Roigé, M., Gómez-Gras, D., Remacha, E., Daza, R., and Boya, S., 2016, Tectonic control on sediment sources in the Jaca basin (Middle and Upper Eocene of the South-Central Pyrenees): Comptes Rendus Geoscience, v. 348, p. 236-245.

Roigé, M., Gómez-Gras, D., Stockli, D. F., Teixell, A., Boya, S., and Remacha, E., 2019, Detrital zircon U–Pb insights into the timing and provenance of the South Pyrenean Jaca basin: Journal of the Geological Society, v. 176, p. 1182-1190.

Sabat, F., Roca, E., Muñoz, J. A., Verges, J., Santanach, P., Masana, E., Sans, M., Estevez, A., and Santiesteban, C., 1995, Role of extension and compression in the evolution of the eastern margin of Iberia: the ESCI-Valencia Trough seismic profile. Revista de la Sociedad Geológica de España, v. 8, p. 431-448.

Saura, E., Ardèvol, L., Teixell, A., and Vergés, J., 2016, Rising and falling diapirs, shifting depocenters, and flap overturning in the Cretaceous Sopeira and Sant Gervàs subbasins (Ribagorça Basin, southern Pyrenees): Tectonics, v. 35, p. 638-662.

Schwartz, T. M., Schwartz, R. K., and Weislogel, A. L., 2019, Orogenic recycling of detrital zircons characterizes age distributions of North American Cordilleran strata. Tectonics, v. 38, 4320-4334.

Sláma, J., Košler, J., Condon, D. J., Crowley, J. L., Gerdes, A., Hanchar, J. M., Horstwood, M. S., Morris, G. A., Nasdala, L., Norberg, N., and Schaltegger, U., 2008, Plešovice zircon—a new natural reference material for U–Pb and Hf isotopic microanalysis: Chemical Geology, v. 249, p. 1-35.

Soler-Sampere, M., and Puigdefàbregas, C., 1970, Líneas generales de la geología del Alto Aragón Occidental.

Steidtmann, J. R., and Schmitt, J. G., 1988, Provenance and dispersal of tectogenic sediments in thin-skinned, thrusted terrains. In New perspectives in basin analysis. Springer, New York, NY.

Tarriño, A., 2006, El sílex en la cuenca vasco cantábrica y pirineo navarro: caracterización y su aprovechamiento en la prehistoria (Doctoral dissertation, Universidad del País Vasco-Euskal Herriko Unibertsitatea).

Teixell, A., 1996, The Ansó transect of the southern Pyrenees: basement and cover thrust geometries: Journal of the Geological Society, v. 153, p. 301-310.

Teixell, A., and García-Sansegundo, J., 1995, Estructura del sector central de la Cuenca de Jaca (Pirineos meridionales): Revista de la Sociedad Geológica de España, v. 8, p. 207-220.

Teixell, A., Labaume, P., Ayarza, P., Espurt, N., De Saint blanquat, M., and Lagabrielle, Y., 2018, Crustal structure and evolution of the Pyrenean-Cantabrian belt: A review and new interpretations from recent concepts and data: Tectonophysics, v. 724, p. 146-170.

Teixell, A., Labaume, P., and Lagabrielle, Y., 2016, The crustal evolution of the west-central Pyrenees revisited: Inferences from a new kinematic scenario: Comptes Rendus Geoscience, v. 348, p. 257-267.

Thomson, K. D., Stockli, D. F., Clark, J. D., Puigdefàbregas, C., and Fildani, A., 2017, Detrital zircon (U-Th)/(He-Pb) double-dating constraints on provenance and foreland basin evolution of the Ainsa Basin, south-central Pyrenees, Spain: Tectonics, v. 36, p. 1352-1375.

Thomson, K. D., Stockli, D. F., Odlum, M. L., Tolentino, P., PUIGDEFÀBREGAS, C., CLARK, J., AND FILDANI, A., 2020, Sediment provenance and routing evolution in the Late Cretaceous–Eocene Ager Basin, south-central Pyrenees, Spain: Basin Research, v. 32, p. 485-504.

Vacherat, A., Mouthereau, F., Pik, R., Huyghe, D., Paquette, J.L., christophoul, F., Loget, N. and Tibari, B., 2017, Rift-to-collision sediment routing in the Pyrenees: A synthesis from sedimentological, geochronological and kinematic constraints: Earth-Science Reviews, v. 172, p. 43-74.

Vergés, J., Fernàndez, M., and Martínez, A., 2002, The Pyrenean orogen: pre-, syn-, and post-collisional evolution. Journal of the Virtual Explorer, v. 8, p. 55-74.

Vermeesch, P., 2004, How many grains are needed for a provenance study?. Earth and Planetary Science Letters, v. 224, p. 441-451.

Vermeesch, P., 2013, Multi-sample comparison of detrital age distributions: Chemical Geology, v. 341, p. 140-146.

Vermeesch, P., Resentini, A., and Garzanti, E., 2016, An R package for statistical provenance analysis: Sedimentary Geology, v. 336, p. 14-25.

Vermeesch, P., 2018, Statistical models for point-counting data. Earth and Planetary Science Letters: v. 501, p. 112-118.

Vinyoles, A., López-Blanco, M., Garcés, M., Arbués, P., Valero, L., Beamud, E., Oliva-Urcia, B. and Cabello, P., 2021, 10 Myr evolution of sedimentation rates in a deep marine to non-marine foreland basin system: Tectonic and sedimentary controls (Eocene, Tremp–Jaca Basin, Southern Pyrenees, NE Spain): Basin Research, v. 33, p. 447-477.

Whitchurch, A. L., Carter, A., Sinclair, H. D., Duller, R. A., Whittaker, A. C., and Allen, P. A., 2011, Sediment routing system evolution within a diachronously uplifting orogen: Insights from detrital zircon thermochronological analyses from the South-Central Pyrenees: American Journal of Science, v. 311, p. 442-482.

Wolfe, M. R., and Stockli, D. F., 2010, Zircon (U–Th)/He thermochronometry in the KTB drill hole, Germany, and its implications for bulk He diffusion kinetics in zircon: Earth and Planetary Science Letters, v. 295, p. 69-82.

FIGURE CAPTIONS

Figure 1. (A) Simplified geological map of the Pyrenees (redrawn from Teixell et al. 1996), showing the location of the study area (grey frames, detailed maps in Fig. 2). Grey line indicates cross-section in Figure 1B. (B) Crustal cross-section of the west-central Pyrenees (simplified from Teixell et al. 2016), showing both the South Pyrenean Zone and the North Pyrenean Zone. SPTF: South Pyrenean Frontal Thrust.

Figure 2. Geological maps of the Jaca basin (modified from Puigdefàbregas 1975). (A) Geological maps of the eastern Jaca basin. (B) Geological maps of the western Jaca basin. Yellow-purple lines show the location of the study sections. Numbers refer to each section: (1) Rodellar section; (2) Bibán section; (3) Monrepós section, (4) Gállego section, (5) Luesia section, (6) Yesa section, and (7) Izaga section. Squares indicate the position of samples collected in alluvial deposits, circles indicate samples from fluvial deposits, triangles refer to samples from deltaic environments, while diamonds indicate turbidite deposits. Black stroke indicates U-Pb samples and white stroke double-dated samples.

Figure 3. General stratigraphic cross-section sketch with symbols and labels representing the relative position of the analyzed samples. Squares indicate the position of samples collected in alluvial deposits, circles indicate samples from fluvial deposits, triangles refer to samples from deltaic environments, while diamonds indicate turbidite deposits. Black stroke indicates U-Pb samples and white stroke double-dated samples.

Figure 4. DZ U-Pb results for the eastern Jaca basin. DZ U-Pb results are represented as Kernel density estimators (Nonadaptative, bandwidth of 8 Ma), histogram diagrams from 0 to 1300 Ma. (Bin width of 20 Ma.), and pie percentage charts.

Figure 5. DZ U-Pb results for the western Jaca basin and Ebro basin. DZ U-Pb results are represented as Kernel density estimators (Non-adaptative, bandwidth of 8 Ma), histogram diagrams from 0 to 1300 Ma. (Bin width of 20 Ma.), and pie percentage charts.

Figure 6. (A and B) MDS of U-Pb ages (C and D) CA of U-Pb age components. Sample shapes refer to a certain provenance/source areas, which are CEPS: Central Eastern Pyrenean sourced; WPS: Western Pyrenean Sourced (Basque massifs or Basque

massifs+Urbasa-Andía Sierra or Urbassa-Andia Sierra); WCPS: West Central Pyrenean Sourced (Eocene Turbidite basin+Internal Sierras+North Pyrenean Zone or Eocene Turbidite basin+Internal Sierras+North Pyrenean Zone+Jaca thrust sheet top basin); WPS+WCPS: Pyrenean Sourced Western Pyrenean Sourced (Basque massifs or Basque massifs+Urbasa-Andía Sierra or Urbassa-Andia Sierra) + West Central Pyrenean Sourced (Eocene Turbidite basin+Internal Sierras+North Pyrenean Zone or Eocene Turbidite basin+Internal Sierras+North Pyrenean Zone+Jaca thrust sheet top basin).

Figure 7. (U-Th)/He results of the analyzed samples represented as pie diagrams and scatterplot of (U-Th)/He age versus U-Pb age for double-dated grains. The main cooling events are abbreviated in each diagram as: P.O. Pyrenean Orogeny; C.R. Cretaceous Rifting; L.C. Liassic Cooling; P.T.R. Permo-Triassic Rifting; V.O. Variscan Orogeny.

Figure 8. (A and B) Multi-Dimensional Scaling (MDS) of (U-Th)/He ages (C and D) Correspondence Analysis (CA) of (U-Th)/He age components. Sample shapes refer to a certain provenance/source areas, which are CEPS: Central Eastern Pyrenean sourced; WPS: Western Pyrenean Sourced (Basque massifs or Basque massifs+Urbasa-Andía Sierra or Urbasa-Andia Sierra); WCPS: West Central Pyrenean Sourced (Eocene Turbidite basin+Internal Sierras+North Pyrenean Zone or Eocene Turbidite basin+Internal Sierras+North Pyrenean Zone+Jaca thrust sheet top basin); WPS+WCPS: Pyrenean Sourced Western Pyrenean Sourced (Basque massifs or Basque massifs+Urbasa-Andía Sierra or Urbasa-Andia Sierra) + West Central Pyrenean Sourced (Eocene Turbidite basin+Internal Sierras+North Pyrenean Zone or Eocene Turbidite basin+Internal Sierras+North Pyrenean Zone+Jaca thrust sheet top basin).

Figure 9. Paleogeographic interpretation of the sediment routing systems functioning of the Jaca basin. (A) During Bartonian times, the eastern Jaca basin was dominated by the Sabinánigo delta to the north, which received from a northern source area rich in sandstone and carbonate rocks and Cadomian-dominated DZ U-Pb signatures (Roige et al. 2023). To the south of the eastern Jaca basin, the Belsué-Atarés delta was sourced from the central Pyrenees which delivered plutonic rock fragments, Variscan-dominated DZ U-Pb ages and Pyrenean cooling ages. In contrast, the western Jaca basin accumulated turbiditic sedimentation derived from the Basque Massifs, which produced abundant feldspar grains, Cadomian-dominated DZ U-Pb signatures and Pre-Pyrenean ZHe cooling ages. (B) During Oligocene times, terrestrial environments dominated the Jaca basin. The eastern sector was dominated by alluvial systems which deeply recycled the former turbidite deposits (Cadomian-dominated DZ U-Pb signatures), while the western sector of the basin concentrated alluvial fans sourced from the Urbasa-Andía Sierras that delivered carbonate rock fragments, Cadomian-dominated DZ U-Pb signatures and Pre-Pyrenean cooling ages. In the Ebro basin, the Luna alluvial fan received contributions from the Basque Massifs and the Eocene foreland deposits (Cadomian-dominated DZ U-Pb signatures and Pyrenean and Pre-Pyrenean ZHe cooling ages).

TABLES

Table 1. Detrital zircon U-Pb results summarized in component percentages.

Table 2. Detrital zircon (U-Th)/He results summarized in component percentages.

SUPPLEMENTARY DATA

S1 List of analysed samples and locations.

S2 Extended Zircon U-Pb LA-ICP-MS methodology.

S3 Reduced detrital zircon U-Pb dataset for all sample analyses.

S4 Reduced detrital zircon double dating (U-Th)/(He-Pb) data for all sample analyses.

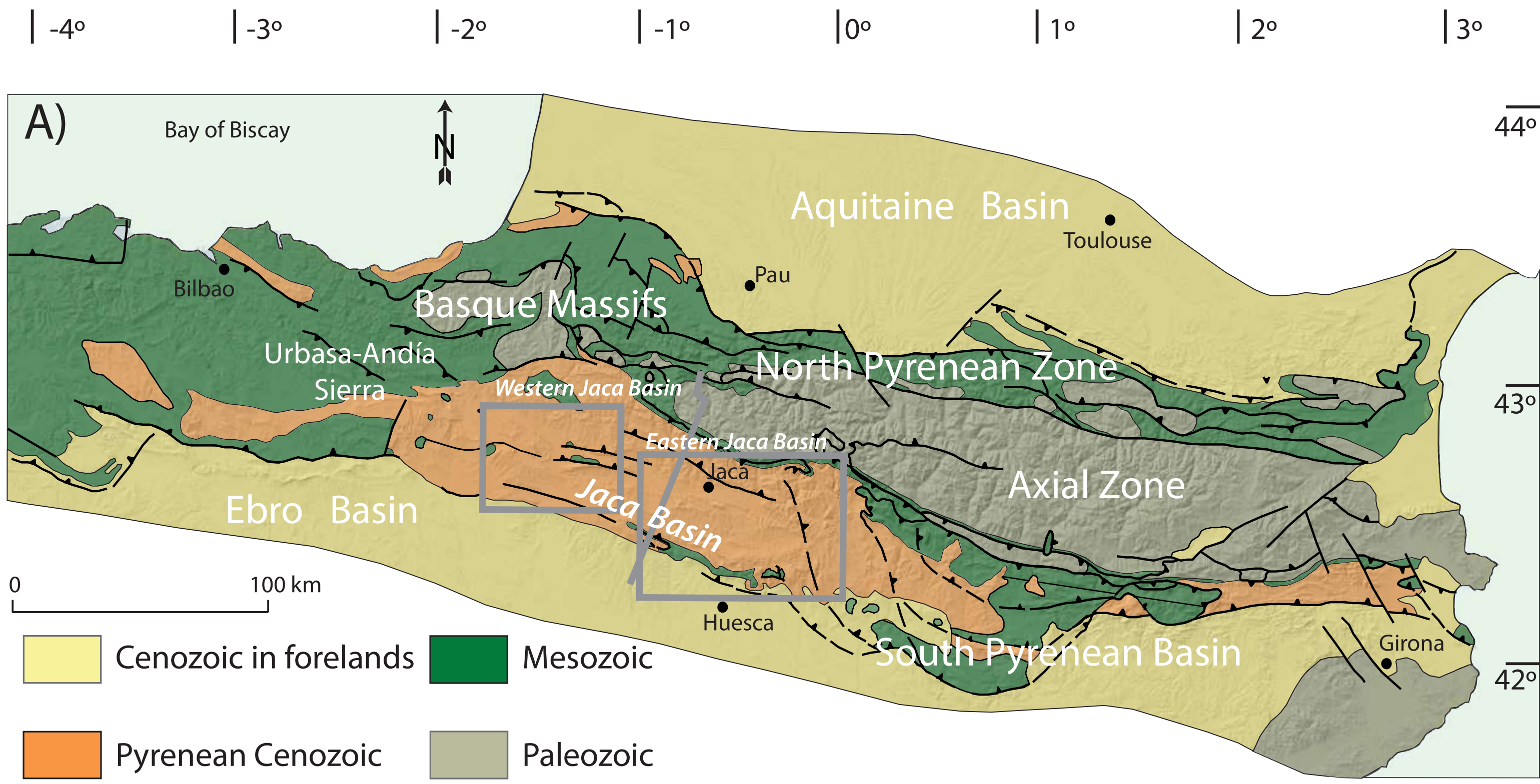

-4º
-3º
-2º
-1º
0º
1º
2º
3º
44º
43º
42º
A)
Bay of Biscay
N
Aquitaine Basin
Toulouse
Pau
Bilbao
Basque Massifs
Urbasa-Andía Sierra
Western Jaca Basin
North Pyrenean Zone
Eastern Jaca Basin
Jaca
Axial Zone
Ebro Basin
Jaca Basin
0
100 km
Huesca
South Pyrenean Basin
Girona
Cenozoic in forelands
Mesozoic
Pyrenean Cenozoic
Paleozoic

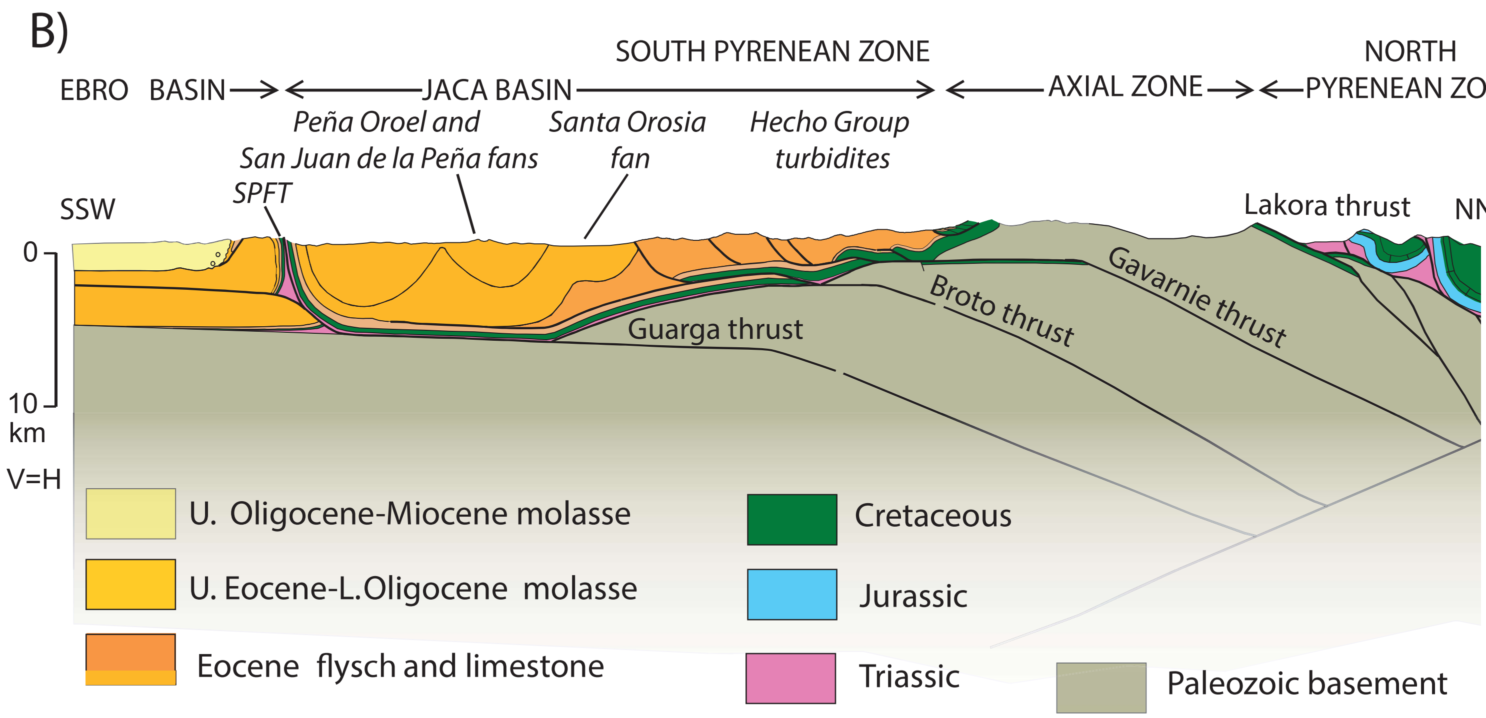

B)
SOUTH PYRENEAN ZONE
NORTH
EBRO BASIN
JACA BASIN
AXIAL ZONE
PYRENEAN ZONE
Peña Oroel and
San Juan de la Peña fans
Santa Orosia
fan
Hecho Group
turbidites
SPFT
SSW
Lakora thrust
NNE
0
10
km
V=H
Gavarnie thrust
Broto thrust
Guarga thrust
U. Oligocene-Miocene molasse
U. Eocene-L.Oligocene molasse
Eocene flysch and limestone
Cretaceous
Jurassic
Triassic
Paleozoic basement

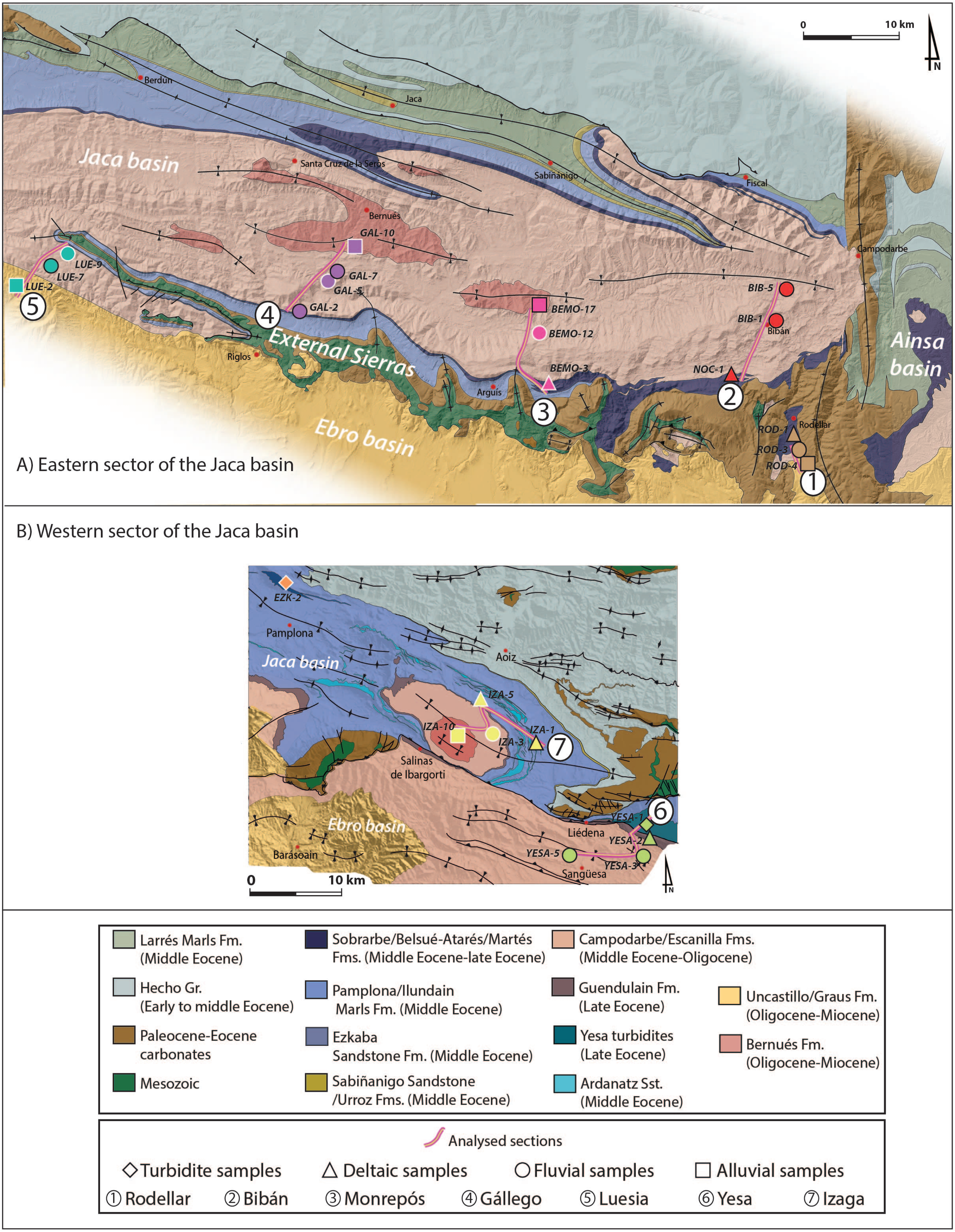

0
10 km
N
Berdún
Jaca
Jaca basin
Santa Cruz de la Serós
Sabiñánigo
Fiscal
Bernués
GAL-10
Campodarbe
LUE-9
LUE-7
LUE-2
GAL-7
GAL-5
GAL-2
BIB-5
BEMO-17
BIB-1
Bibán
BEMO-12
External Sierras
Riglos
BEMO-3
NOC-1
Arguís
Ainsa basin
Rodellar
ROD-1
ROD-3
ROD-4
Ebro basin
A) Eastern sector of the Jaca basin
B) Western sector of the Jaca basin
EZK-2
Pamplona
Aoiz
IZA-5
IZA-10
IZA-1
IZA-3
Salinas de Ibargorti
YESA-1
Liédena
YESA-2
YESA-5
YESA-3
Sangüesa
Barásoain
Larrés Marls Fm. (Middle Eocene)
Hecho Gr. (Early to middle Eocene)
Paleocene-Eocene carbonates
Mesozoic
Sobrarbe/Belsué-Atarés/Martés Fms. (Middle Eocene-late Eocene)
Pamplona/Ilundain Marls Fm. (Middle Eocene)
Ezkaba Sandstone Fm. (Middle Eocene)
Sabiñanigo Sandstone /Urroz Fms. (Middle Eocene)
Campodarbe/Escanilla Fms. (Middle Eocene-Oligocene)
Guendulain Fm. (Late Eocene)
Yesa turbidites (Late Eocene)
Ardanatz Sst. (Middle Eocene)
Uncastillo/Graus Fm. (Oligocene-Miocene)
Bernués Fm. (Oligocene-Miocene)
Analysed sections
Turbidite samples
Deltaic samples
Fluvial samples
Alluvial samples
① Rodellar
② Bibán
③ Monrepós
④ Gállego
⑤ Luesia
⑥ Yesa
⑦ Izaga

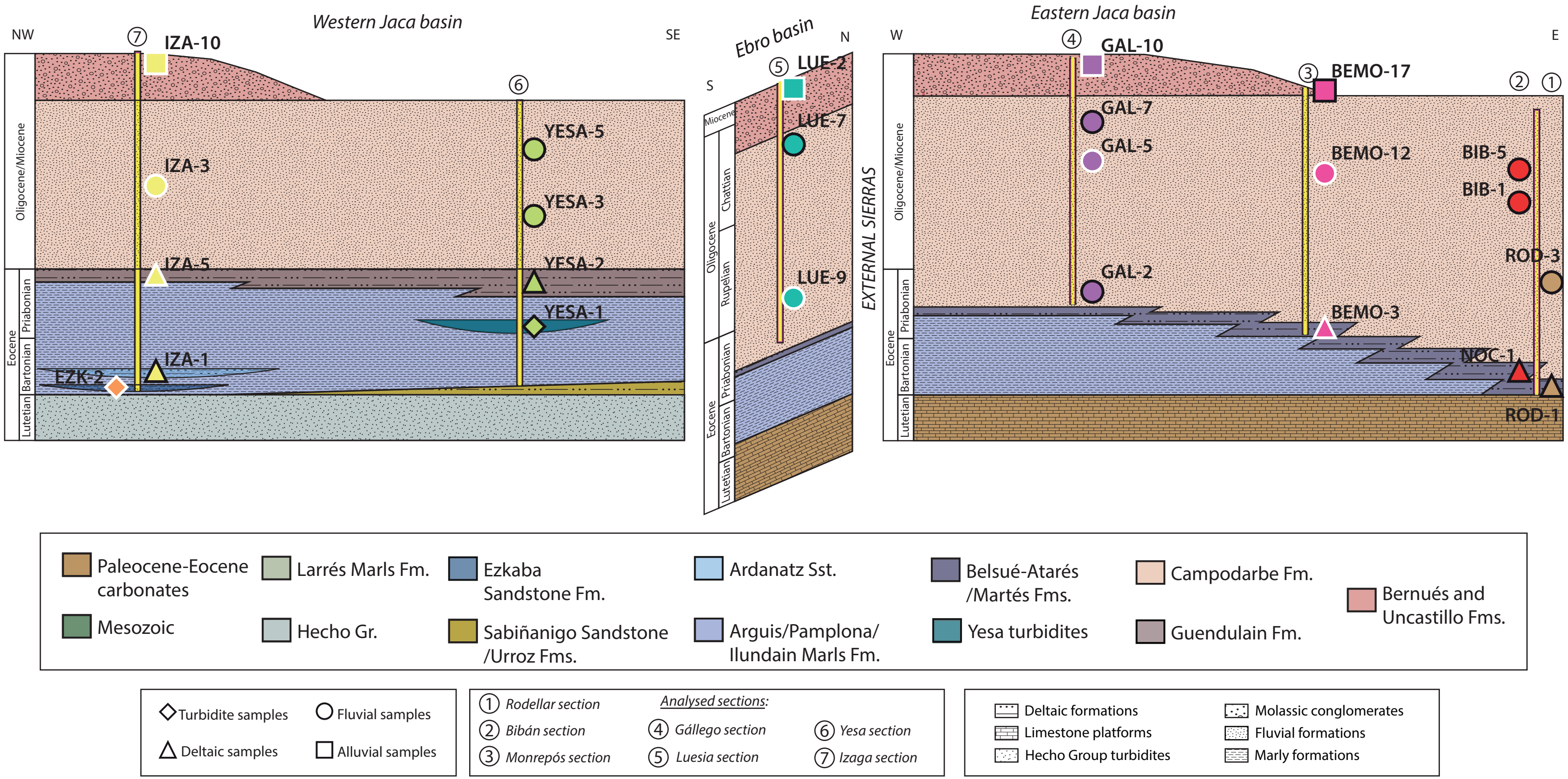

Western Jaca basin
NW
SE
IZA-10
IZA-3
IZA-5
IZA-1
EZK-2
YESA-5
YESA-3
YESA-2
YESA-1
Oligocene/Miocene
Eocene
Priabonian
Bartonian
Lutetian
Ebro basin
S
N
LUE-2
LUE-7
LUE-9
Miocene
Oligocene
Chattian
Rupelian
Eocene
Priabonian
Bartonian
Lutetian
EXTERNAL SIERRAS
Eastern Jaca basin
W
E
GAL-10
GAL-7
GAL-5
GAL-2
BEMO-17
BEMO-12
BEMO-3
BIB-5
BIB-1
ROD-3
ROD-1
NOC-1
Paleocene-Eocene carbonates
Larrés Marls Fm.
Ezkaba Sandstone Fm.
Ardanatz Sst.
Belsué-Atarés /Martés Fms.
Campodarbe Fm.
Bernués and Uncastillo Fms.
Mesozoic
Hecho Gr.
Sabiñanigo Sandstone /Urroz Fms.
Arguis/Pamplona/ Ilundain Marls Fm.
Yesa turbidites
Guendulain Fm.
Turbidite samples
Fluvial samples
Deltaic samples
Alluvial samples
Analysed sections:
① Rodellar section
② Bibán section
③ Monrepós section
④ Gállego section
⑤ Luesia section
⑥ Yesa section
⑦ Izaga section
Deltaic formations
Limestone platforms
Hecho Group turbidites
Molassic conglomerates
Fluvial formations
Marly formations

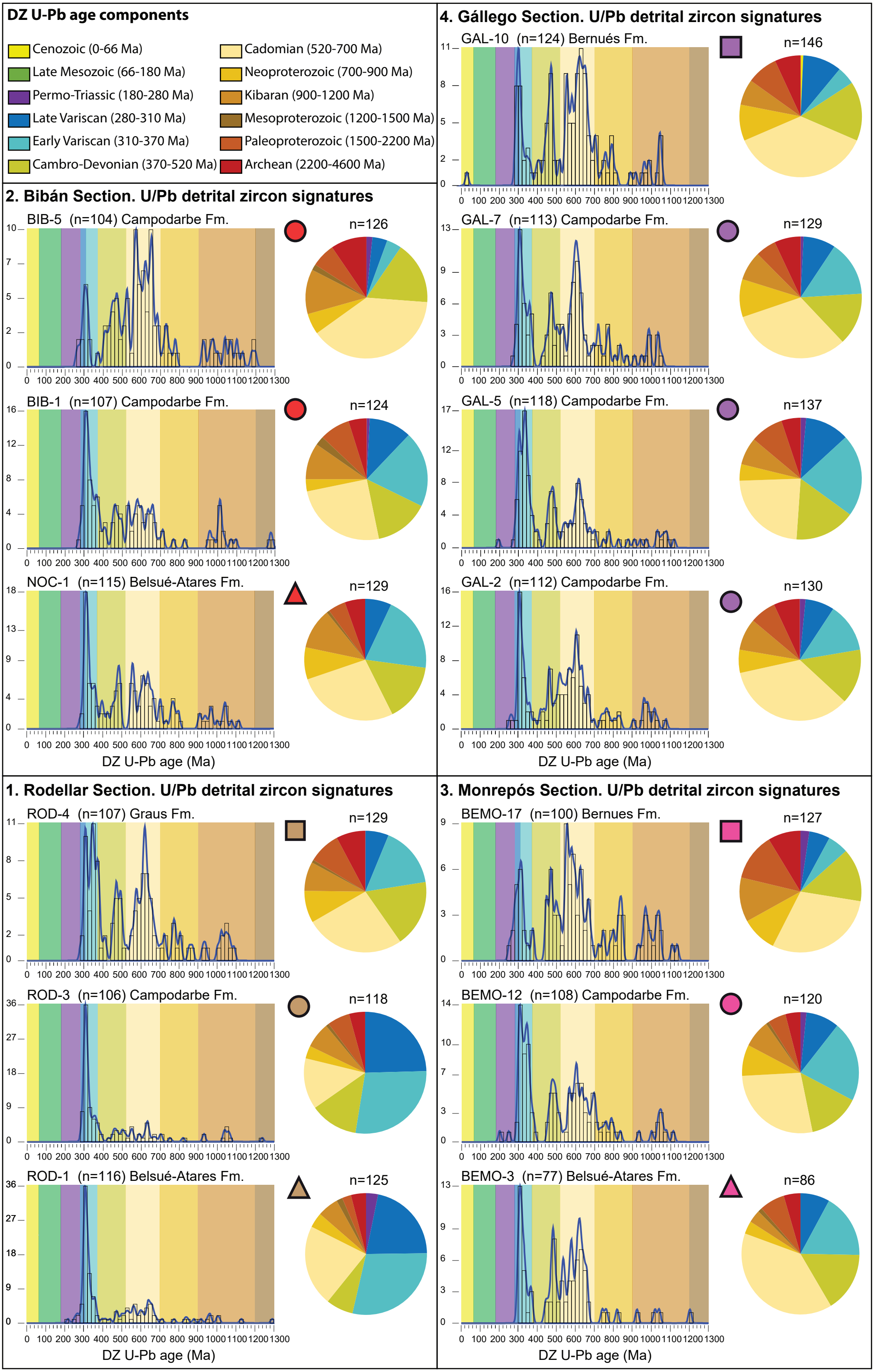

DZ U-Pb age components
Cenozoic (0-66 Ma)
Late Mesozoic (66-180 Ma)
Permo-Triassic (180-280 Ma)
Late Variscan (280-310 Ma)
Early Variscan (310-370 Ma)
Cambro-Devonian (370-520 Ma)
Cadomian (520-700 Ma)
Neoproterozoic (700-900 Ma)
Kibaran (900-1200 Ma)
Mesoproterozoic (1200-1500 Ma)
Paleoproterozoic (1500-2200 Ma)
Archean (2200-4600 Ma)
4. Gállego Section. U/Pb detrital zircon signatures
GAL-10 (n=124) Bernués Fm.
n=146
GAL-7 (n=113) Campodarbe Fm.
n=129
GAL-5 (n=118) Campodarbe Fm.
n=137
GAL-2 (n=112) Campodarbe Fm.
n=130
2. Bibán Section. U/Pb detrital zircon signatures
BIB-5 (n=104) Campodarbe Fm.
n=126
BIB-1 (n=107) Campodarbe Fm.
n=124
NOC-1 (n=115) Belsué-Atares Fm.
n=129
DZ U-Pb age (Ma)
1. Rodellar Section. U/Pb detrital zircon signatures
ROD-4 (n=107) Graus Fm.
n=129
ROD-3 (n=106) Campodarbe Fm.
n=118
ROD-1 (n=116) Belsué-Atares Fm.
n=125
3. Monrepós Section. U/Pb detrital zircon signatures
BEMO-17 (n=100) Bernues Fm.
n=127
BEMO-12 (n=108) Campodarbe Fm.
n=120
BEMO-3 (n=77) Belsué-Atares Fm.
n=86
DZ U-Pb age (Ma)
0 100 200 300 400 500 600 700 800 900 1000 1100 1200 1300

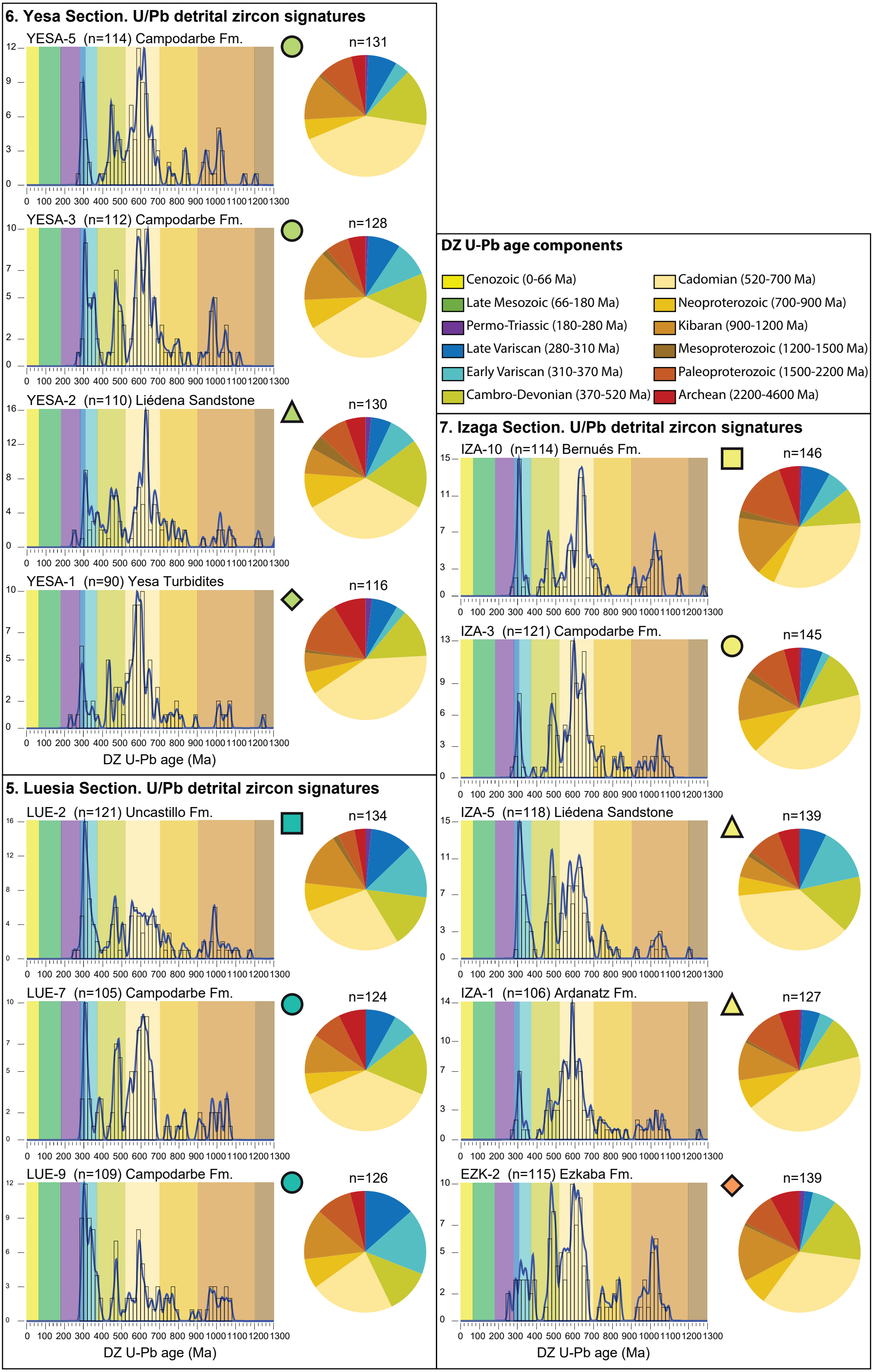

6. Yesa Section. U/Pb detrital zircon signatures
YESA-5 (n=114) Campodarbe Fm.
n=131
YESA-3 (n=112) Campodarbe Fm.
n=128
YESA-2 (n=110) Liédena Sandstone
n=130
YESA-1 (n=90) Yesa Turbidites
n=116
DZ U-Pb age (Ma)
5. Luesia Section. U/Pb detrital zircon signatures
LUE-2 (n=121) Uncastillo Fm.
n=134
LUE-7 (n=105) Campodarbe Fm.
n=124
LUE-9 (n=109) Campodarbe Fm.
n=126
DZ U-Pb age (Ma)
DZ U-Pb age components
Cenozoic (0-66 Ma)
Late Mesozoic (66-180 Ma)
Permo-Triassic (180-280 Ma)
Late Variscan (280-310 Ma)
Early Variscan (310-370 Ma)
Cambro-Devonian (370-520 Ma)
Cadomian (520-700 Ma)
Neoproterozoic (700-900 Ma)
Kibaran (900-1200 Ma)
Mesoproterozoic (1200-1500 Ma)
Paleoproterozoic (1500-2200 Ma)
Archean (2200-4600 Ma)
7. Izaga Section. U/Pb detrital zircon signatures
IZA-10 (n=114) Bernués Fm.
n=146
IZA-3 (n=121) Campodarbe Fm.
n=145
IZA-5 (n=118) Liédena Sandstone
n=139
IZA-1 (n=106) Ardanatz Fm.
n=127
EZK-2 (n=115) Ezkaba Fm.
n=139
DZ U-Pb age (Ma)

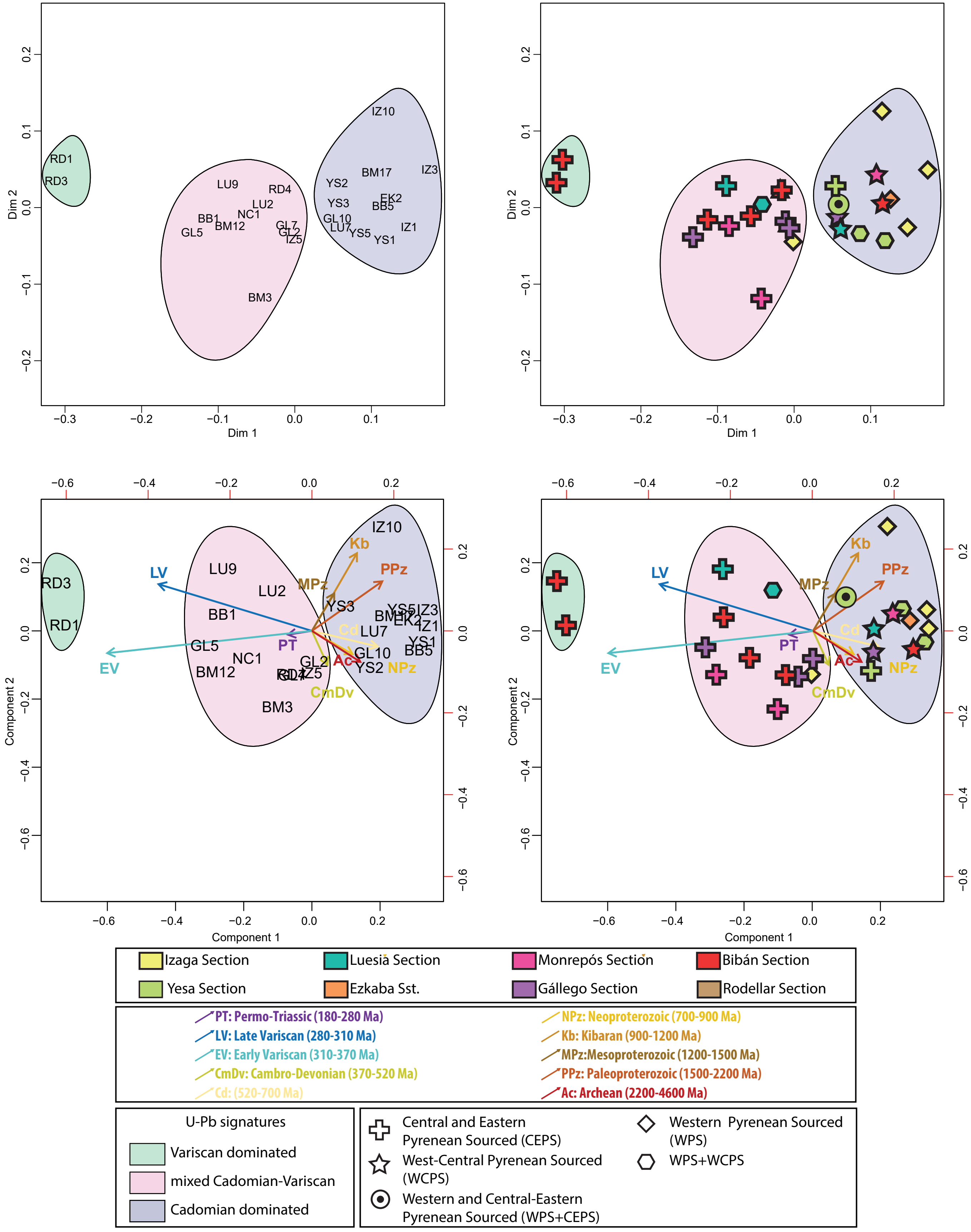
Dim 1
Dim 2
Component 1
Component 2
RD1
RD3
LU9
RD4
LU2
NC1
BB1
BM12
GL5
GL7
GL2
IZ5
BM3
IZ10
YS2
BM17
IZ3
YS3
EK2
BB5
GL10
LU7
YS5
YS1
IZ1
LV
EV
PT
MPz
Kb
PPz
Cd
Ac
NPz
CmDv
Izaga Section
Luesia Section
Monrepós Section
Bibán Section
Yesa Section
Ezkaba Sst.
Gállego Section
Rodellar Section
PT: Permo-Triassic (180-280 Ma)
LV: Late Variscan (280-310 Ma)
EV: Early Variscan (310-370 Ma)
CmDv: Cambro-Devonian (370-520 Ma)
Cd: (520-700 Ma)
NPz: Neoproterozoic (700-900 Ma)
Kb: Kibaran (900-1200 Ma)
MPz:Mesoproterozoic (1200-1500 Ma)
PPz: Paleoproterozoic (1500-2200 Ma)
Ac: Archean (2200-4600 Ma)
U-Pb signatures
Variscan dominated
mixed Cadomian-Variscan
Cadomian dominated
Central and Eastern Pyrenean Sourced (CEPS)
West-Central Pyrenean Sourced (WCPS)
Western and Central-Eastern Pyrenean Sourced (WPS+CEPS)
Western Pyrenean Sourced (WPS)
WPS+WCPS

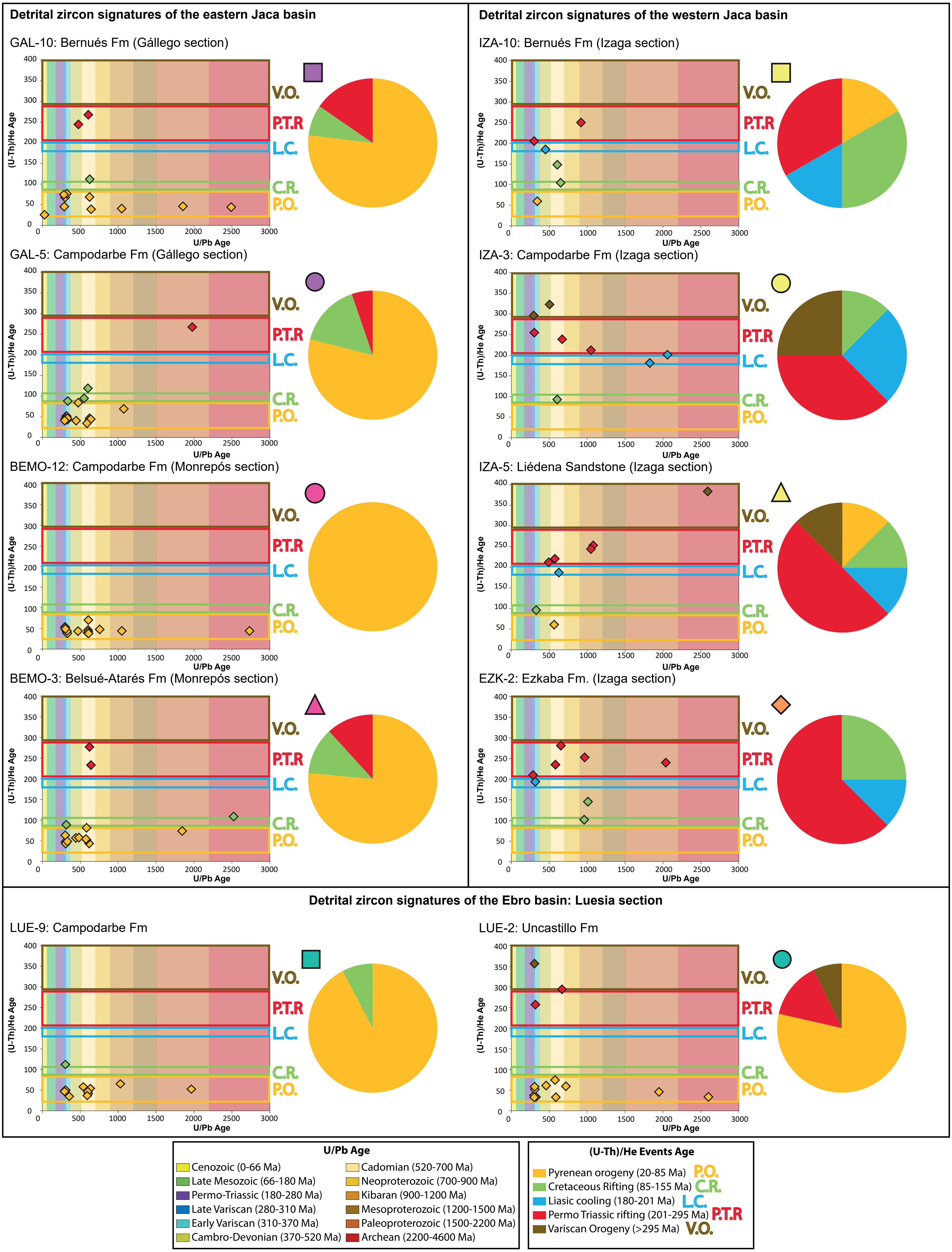
Detrital zircon signatures of the eastern Jaca basin
GAL-10: Bernués Fm (Gállego section)
GAL-5: Campodarbe Fm (Gállego section)
BEMO-12: Campodarbe Fm (Monrepós section)
BEMO-3: Belsué-Atarés Fm (Monrepós section)
Detrital zircon signatures of the western Jaca basin
IZA-10: Bernués Fm (Izaga section)
IZA-3: Campodarbe Fm (Izaga section)
IZA-5: Liédena Sandstone (Izaga section)
EZK-2: Ezkaba Fm. (Izaga section)
Detrital zircon signatures of the Ebro basin: Luesia section
LUE-9: Campodarbe Fm
LUE-2: Uncastillo Fm
(U-Th)/He Age
U/Pb Age
V.O.
P.T.R
L.C.
C.R.
P.O.
U/Pb Age
Cenozoic (0-66 Ma)
Late Mesozoic (66-180 Ma)
Permo-Triassic (180-280 Ma)
Late Variscan (280-310 Ma)
Early Variscan (310-370 Ma)
Cambro-Devonian (370-520 Ma)
Cadomian (520-700 Ma)
Neoproterozoic (700-900 Ma)
Kibaran (900-1200 Ma)
Mesoproterozoic (1200-1500 Ma)
Paleoproterozoic (1500-2200 Ma)
Archean (2200-4600 Ma)
(U-Th)/He Events Age
Pyrenean orogeny (20-85 Ma) P.O.
Cretaceous Rifting (85-155 Ma) C.R.
Liasic cooling (180-201 Ma) L.C.
Permo Triassic rifting (201-295 Ma) P.T.R
Variscan Orogeny (>295 Ma) V.O.

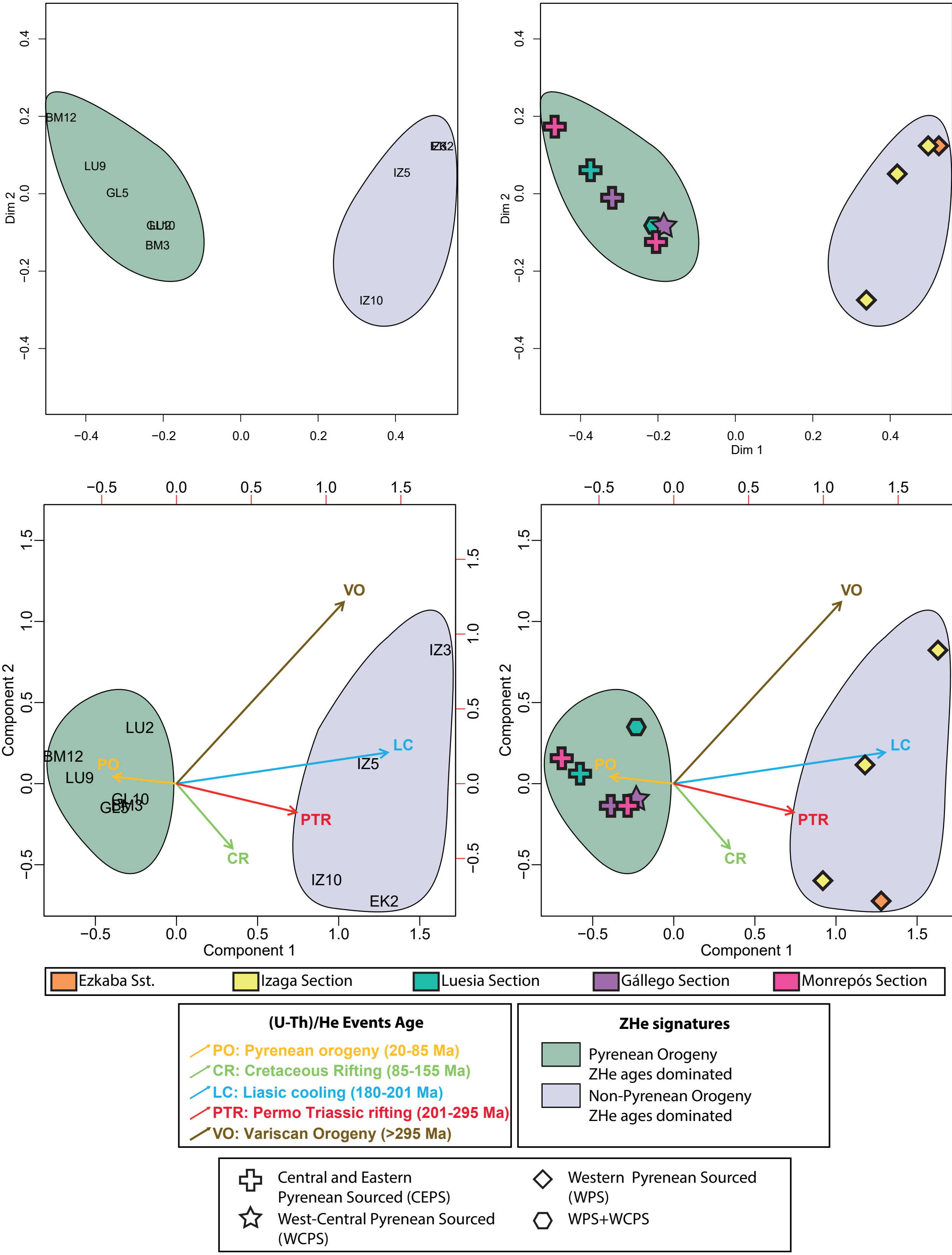

BM12
LU9
GL5
GL10
LU2
BM3
IZ3
EK2
IZ5
IZ10
Dim 1
Dim 2
Component 1
Component 2
VO
LC
PO
PTR
CR
Ezkaba Sst.
Izaga Section
Luesia Section
Gállego Section
Monrepós Section
(U-Th)/He Events Age
PO: Pyrenean orogeny (20-85 Ma)
CR: Cretaceous Rifting (85-155 Ma)
LC: Liasic cooling (180-201 Ma)
PTR: Permo Triassic rifting (201-295 Ma)
VO: Variscan Orogeny (>295 Ma)
ZHe signatures
Pyrenean Orogeny ZHe ages dominated
Non-Pyrenean Orogeny ZHe ages dominated
Central and Eastern Pyrenean Sourced (CEPS)
West-Central Pyrenean Sourced (WCPS)
Western Pyrenean Sourced (WPS)
WPS+WCPS


A
Basque Massifs
(Paleozoic exhumed)
K
CE
P
North Pyrenean Zone
N
Former Eocene
turbiditic wedge
Future Axial Zone
(Initial growth)
Paleozoic basement
not exhumed yet
PrP
Cad
Blind Thrust front
Shoreline
Pamplona
Ezkaba Sandstone
turbidites
Jaca basin
Uplifting area
Sabiñánigo
Sandstone delta
Yesa
Jaca
CE
Snd
Cad
Echauri Sandstone
Q
Santo Domingo
carbonate platform
Belsué-Atarés delta
Ebro basin
Biel
Var
Pyr
CE
PRF
Bartonian
10 km
B
Basque Massifs
(Paleozoic exhumed)
K
CE
P
Urbasa-Andía
Sierra
PrP
Cad
Snd
North Pyrenean Zone
N
Former Eocene
turbiditic wedge
Axial Zone
CE
CE
Cad
PrP
Basement cutoff Guarga thrust
Paleozoic basement
not exhumed yet
Pamplona
Snd
CE
Snd
CE
Uplifting area
El Perdón fan
Izaga fan
Jaca piggy-back basin
Yesa
Cad
Jaca
Cad
Peña Oroel fan
San Juan de la
Peña fan
Cad
MPP
Biel
External Sierras
Ebro basin
Oligocene
10 km
Type of grains supplied from source areas
CE Carbonate extrabasinal grains
K K-feldspar grains
Q Quartz grains
P Plagioclase grains
Snd Sandstone rock fragments
PRF Plutonic rock fragments
Geo- and thermochronological data from detrital zircons
Var Variscan dominated DZ U-Pb
Pyr Pyrenean cooling (ZHe)
Cad Cadomian dominated DZ U-Pb
PrP Pre-pyrenean cooling (ZHe)
Sediment supply
MPP Mixed Pyrenean and Pre-pyrenean cooling (ZHe)

Sample	Formation	n	Cenozoic 0-66 Ma	Late Mesozoic 66-180 Ma	Permo-Triassic 180-280 Ma	Late Variscan 280-310 Ma	Early Variscan 310-370 Ma
RD1	Belsué-Atarés Fm.	126	0.0	0.0	3.2	21.4	29.4
RD3	Campodarbe Fm.	118	0.0	0.0	0.0	24.6	28.0
RD4	Graus Fm.	129	0.0	0.0	0.0	6.2	16.3
NC1	Belsué-Atarés Fm.	131	0.0	0.0	0.8	7.6	19.8
BB1	Campodarbe Fm.	125	0.0	0.0	0.8	11.2	20.0
BB5	Campodarbe Fm.	126	0.0	0.0	1.6	4.0	4.0
BM3	Belsué-Atarés Fm.	87	0.0	0.0	0.0	8.0	17.2
BM12	Campodarbe Fm.	121	0.0	0.0	1.7	9.1	22.3
BM17	Bernués Fm.	127	0.0	0.0	2.4	5.5	5.5
GL2	Campodarbe Fm.	130	0.0	0.0	1.5	7.7	13.1
GL5	Campodarbe Fm.	139	0.0	0.0	1.4	11.5	21.6
GL7	Campodarbe Fm.	129	0.0	0.0	0.8	8.5	14.7
GL10	Bernués Fm.	146	0.7	0.0	0.0	10.3	4.8
LU9	Campodarbe Fm.	127	0.0	0.0	0.0	13.4	18.9
LU7	Campodarbe Fm.	125	0.0	0.0	0.0	8.0	6.4
LU2	Uncastillo Fm.	134	0.0	0.0	1.5	11.2	14.2
YS1	Yesa turbidites	116	0.0	0.0	1.7	6.9	2.6
YS2	Liédena Sst.	130	0.0	0.0	1.5	5.4	7.7
YS3	Campodarbe Fm.	128	0.0	0.0	0.8	8.6	9.4
YS5	Campodarbe Fm.	130	0.0	0.0	0.8	7.7	3.8
EK2	Ezkaba Fm.	139	0.0	0.0	1.4	2.2	6.5
IZ1	Ardanatz Sst.	128	0.0	0.0	0.8	4.7	3.9
IZ5	Liédena Sst.	140	0.0	0.0	0.0	7.1	14.3
IZ3	Campodarbe Fm.	145	0.0	0.0	0.7	5.5	2.8
IZ10	Bernués Fm.	146	0.0	0.0	0.7	7.5	6.2

Cambro-Devonian 370-520 Ma	Cadomian 520-700 Ma	Neo-proterozoic 700-900 Ma	Kibaran 900-1200 Ma	Meso-proterozoic 1200-1500 Ma	Paleo-proterozoic 1500-2200 Ma	Archean 2200-4600 Ma
7.9	21.4	4.0	4.8	1.6	2.4	4.0
12.7	13.6	3.4	6.8	0.8	5.9	4.2
17.8	26.4	8.5	7.8	0.8	8.5	7.8
15.3	26.7	8.4	10.7	0.8	4.6	5.3
15.2	24.8	3.2	9.6	2.4	8.0	4.8
16.7	38.9	5.6	11.9	1.6	6.3	9.5
17.2	39.1	3.4	3.4	1.1	5.7	4.6
14.0	27.3	8.3	7.4	0.8	5.0	4.1
14.2	29.9	9.4	11.8	0.0	11.8	9.4
14.6	34.6	6.2	8.5	0.0	6.9	6.9
16.5	23.0	5.0	7.2	0.0	8.6	5.0
14.0	31.8	10.1	7.8	0.0	5.4	7.0
15.8	37.0	9.6	6.8	0.0	8.2	6.8
11.8	22.0	7.1	13.4	0.0	9.4	3.9
16.8	36.8	5.6	11.2	0.0	8.0	7.2
14.2	27.6	7.5	14.2	1.5	5.2	3.0
12.9	41.4	6.0	5.2	0.9	13.8	8.6
18.5	33.8	9.2	6.9	3.8	7.7	5.4
13.3	34.4	7.8	13.3	1.6	6.3	4.7
15.4	41.5	5.4	11.5	0.8	9.2	3.8
17.3	33.1	7.2	15.1	0.7	9.4	7.2
11.7	43.8	7.8	10.2	0.8	10.9	5.5
15.7	36.4	5.0	5.7	1.4	8.6	5.7
13.1	41.4	9.0	11.7	2.1	9.7	4.1
9.6	32.9	4.8	15.8	2.1	15.1	5.5

Sample	Formation	Section	n	Pyrenean Orogeny (20-85 Ma)	Cretaceous Rifting (85-155 Ma)
BM3	Belsué-Atarés Fm.	Monrepós	17	76.5	11.8
BM12	Campodarbe Fm.	Monrepós	16	100.0	0.0
GL5	Campodarbe Fm.	Gállego	19	78.9	15.8
GL10	Bernués Fm.	Gállego	13	76.9	7.7
LU9	Campodarbe Fm.	Luesia	13	92.3	7.7
LU2	Uncastillo Fm.	Luesia	14	78.6	0.0
EK2	Ezkaba Fm.	Izaga	8	0.0	25.0
IZ5	Liédena Sst.	Izaga	8	12.5	12.5
IZ3	Campodarbe Fm.	Izaga	8	0.0	12.5
IZ10	Bernués Fm.	Izaga	6	16.7	33.3

Liasic Cooling (180-201 Ma)	Permo-Triassic Rifting (201-295 Ma)	Variscan Orogeny (>295 Ma)
0.0	11.8	0.0
0.0	0.0	0.0
0.0	5.3	0.0
0.0	15.4	0.0
0.0	0.0	0.0
0.0	14.3	7.1
12.5	62.5	0.0
12.5	50.0	12.5
25.0	37.5	25.0
16.7	33.3	0.0